Specific tyrosine phosphorylation sites on cortactin regulate Nck1-dependent actin polymerization in invadopodia

Matthew Oser[1,2,*], Christopher C. Mader[3,4,*], Hava Gil-Henn[4], Marco Magalhaes[1,2], Jose Javier Bravo-Cordero[1,2], Anthony J. Koleske[4,‡] and John Condeelis[1,2,‡]

[1]Department of Anatomy and Structural Biology and [2]Gruss Lipper Biophotonics Center, Albert Einstein College of Medicine of Yeshiva University, Bronx, NY 10461, USA
[3]Department of Cell Biology and [4]Department of Molecular Biophysics and Biochemistry, Yale University, 333 Cedar Street, New Haven, CT 06520, USA

*These authors contributed equally to this work
‡Authors for correspondence (anthony.koleske@yale.edu; john.condeelis@einstein.yu.edu)

Accepted 27 July 2010
Journal of Cell Science 123, 3662-3673

doi:10.1242/jcs.068163

Summary

Invadopodia are matrix-degrading membrane protrusions in invasive carcinoma cells enriched in proteins that regulate actin polymerization. The on–off regulatory switch that initiates actin polymerization in invadopodia requires phosphorylation of tyrosine residues 421, 466, and 482 on cortactin. However, it is unknown which of these cortactin tyrosine phosphorylation sites control actin polymerization. We investigated the contribution of individual tyrosine phosphorylation sites (421, 466, and 482) on cortactin to the regulation of actin polymerization in invadopodia. We provide evidence that the phosphorylation of tyrosines 421 and 466, but not 482, is required for the generation of free actin barbed ends in invadopodia. In addition, these same phosphotyrosines are important for Nck1 recruitment to invadopodia via its SH2 domain, for the direct binding of Nck1 to cortactin in vitro, and for the FRET interaction between Nck1 and cortactin in invadopodia. Furthermore, matrix proteolysis-dependent tumor cell invasion is dramatically inhibited in cells expressing a mutation in phosphotyrosine 421 or 466. Together, these results identify phosphorylation of tyrosines 421 and 466 on cortactin as the crucial residues that regulate Nck1-dependent actin polymerization in invadopodia and tumor cell invasion, and suggest that specifically blocking either tyrosine 421 or 466 phosphorylation might be effective at inhibiting tumor cell invasion in vivo.

Key words: Invadopodia, Cortactin, Nck1, Phosphorylation, SH2, Cancer invasion

Introduction

Tumor metastasis, the spreading of cancer from a primary site to a distant organ, initially requires the tumor cell to successfully invade the basement membrane underlying the epithelium and intravasate through the basement membrane of the endothelium into the bloodstream (Condeelis and Segall, 2003). It is thought that invasive tumor cells use subcellular structures known as invadopodia to degrade through basement membranes during invasion and intravasation (Poincloux et al., 2009; Schoumacher et al., 2010; Weaver, 2008). Invadopodia are actin-rich membrane protrusions specifically present in metastatic carcinoma cells (Yamaguchi et al., 2005) that have the ability to focally degrade the extracellular matrix (ECM) using matrix metalloproteinase (MMP) activity (Weaver, 2008). Invadopodia develop through a series of maturation events, beginning with the formation of the invadopodium precursor (Artym et al., 2006) and followed by actin polymerization (Oser et al., 2009), before acquiring the ability to efficiently degrade the ECM. Regulating actin polymerization by controlling the concentration of free barbed ends in invadopodia is not required for invadopodium precursor formation, but is crucial for invadopodium maturation (Oser et al., 2009) and for tumor metastasis in vivo (Wang et al., 2006).

The cortactin protein promotes invadopodium precursor formation and matrix degradation in many cancer cell types (Artym et al., 2006; Ayala et al., 2008; Oser et al., 2009) and breast cancer metastasis in animal models (Li et al., 2001). Cortactin regulates actin polymerization (Oser et al., 2009) and MMP recruitment and secretion in invadopodia (Clark et al., 2007) resulting in proper invadopodium maturation. After initial assembly of the invadopodium precursor, cortactin phosphorylation at three tyrosine residues (421, 466, and 482) is crucial for the generation of free actin barbed ends for actin polymerization in invadopodia. The mechanism by which cortactin tyrosine phosphorylation regulates actin polymerization in invadopodia involves: first, direct binding of cofilin to cortactin, thereby regulating the severing activity of cofilin; and second, recruitment and binding of NcK1 to cortactin, thereby activating a Nck1–N-WASp pathway leading to Arp2/3-complex-dependent actin polymerization (Oser et al., 2009). Regulation of both cofilin and Nck1 recruitment via cortactin tyrosine phosphorylation is required for successful maturation from an invadopodium precursor to a matrix-degrading invadopodium (Oser et al., 2009; Yamaguchi et al., 2005). However, how the specific cortactin tyrosine phosphorylation sites (421, 466 and 482) that engage these distinct pathways to regulate actin polymerization in invadopodia is unknown.

Cortactin phosphorylation promotes its binding to Nck1, an adaptor protein that activates N-WASp to stimulate Arp2/3 complex-mediated actin filament nucleation (Tehrani et al., 2007). Phospho-cortactin interactions with a Nck1–N-WASp–Arp2/3 assembly complex is essential for efficient actin polymerization in

the invadopodia of mammary carcinoma cells (Oser et al., 2009) and in actin-based cell edge protrusions in fibroblasts (Lapetina et al., 2009). Together, these studies provide strong evidence that pathways involving cortactin tyrosine phosphorylation and Nck1 are essential for actin polymerization in various motility processes involving the actin cytoskeleton. However, it is unclear which of the specific phosphotyrosines on cortactin (421, 466 or 482) initiates Nck1 recruitment leading to the activation of the Arp2/3 complex. Given the documented specificity of interaction between SH2 domains and phosphotyrosine-containing peptide sequences (Machida et al., 2007), it is likely that Nck1 binds preferentially to a specific phosphotyrosine on cortactin for Nck1 recruitment to invadopodia, leading to activation of N-WASp-dependent actin polymerization.

Here, we have investigated the contribution of individual cortactin phosphorylation sites in regulating actin polymerization in invadopodia. We provide evidence that the phosphorylation of tyrosines 421 and 466, but not 482, regulates the number of free barbed ends in invadopodia, recruitment of Nck1 to invadopodia via its SH2 domain, and are crucial for the cortactin–Nck1 direct binding interaction in vitro and for the cortactin–Nck1 fluorescence resonance energy transfer (FRET) interaction in invadopodia. Furthermore, matrix proteolysis-dependent tumor cell invasion is dramatically inhibited in cells expressing a mutation in phosphotyrosine 421 or 466. Together, these results identify tyrosines 421 and 466 as the preferred phospho-residues that regulate Nck1-dependent actin polymerization in invadopodia and tumor cell invasion.

Results

To determine the specific role for cortactin tyrosine phosphorylation sites during invadopodium maturation, stable human MDA-MB-231 breast carcinoma cell lines were engineered to express cortactin–TagRFP tyrosine phosphorylation mutants containing single tyrosine (Y) to phenylalanine (F) point mutations in tyrosine phosphorylation sites 421, 466 and 482, or containing 466/482 or 421/482 double point mutations (supplementary material Fig. S1A). Using these cell lines, endogenous cortactin was transiently knocked down using human specific siRNA yielding ~90% knockdown between 72 and 96 hours after transfection; during this time window, the cell lines solely express murine cortactin–TagRFP phospho-mutant constructs (supplementary material Fig. S1A–C). These cell lines stably expressing cortactin–TagRFP mutants with transient knockdown of endogenous cortactin were used for all experiments.

To confirm the absence of tyrosine phosphorylation on the specific tyrosine residues that were mutated to phenylalanine, the cell lines were stimulated with pervanadate, and cell lysates were immunoblotted using phosphospecific antibodies against either tyrosine 421 or 466. The absence of tyrosine phosphorylation at the specific mutated tyrosine residues confirms that the approach was successful (supplementary material Fig. S1D).

Cortactin phosphorylation of tyrosines 421 and 466, but not 482, is required for actin polymerization in invadopodia

Epidermal growth factor (EGF) stimulation activates downstream signaling pathways, resulting in an increase of free actin filament barbed ends and subsequent actin polymerization in invadopodia in rat metastatic mammary carcinoma cells (Oser et al., 2009; Yamaguchi et al., 2005). To determine whether EGF induces the generation of free actin barbed ends in invadopodia of MDA-MB-231 cells, we measured free barbed end intensity in invadopodia of cells expressing cortactin WT–TagRFP at various times after stimulation, as described previously (Chan et al., 1998; Oser et al., 2009). A clear peak of free actin barbed ends formed in invadopodium precursors 3 minutes after EGF stimulation (Fig. 1A). To confirm that barbed ends are also enriched in matrix-degrading invadopodia, we repeated the assay using cells plated on Alexa Fluor 405–gelatin. Barbed ends were also enriched in invadopodia actively degrading matrix, identified by focal reduction or clearing of the Alexa Fluor 405–gelatin signal (Fig. 1B).

We hypothesized that specific cortactin tyrosine phosphorylation sites mediate the EGF-induced increase in barbed ends in invadopodia. To test this, free actin barbed ends were analyzed in various cortactin–TagRFP phosphorylation site mutant-expressing MDA-MB-231 cell lines with endogenous cortactin knocked down. Cells expressing cortactin Y3F–TagRFP, Y421F–TagRFP, and Y466F–TagRFP, but not cells expressing cortactin WT–TagRFP or Y482F–TagRFP, were defective in generating barbed ends in response to EGF at invadopodium precursors (Fig. 1C,D). As previously reported for MTLn3 cells, invadopodium precursors form normally in all cortactin–TagRFP mutant-expressing MDA-MB-231 cell lines (Fig. 1E). These data affirm that cortactin tyrosine phosphorylation and barbed end formation are not essential for initial assembly of invadopodium precursors in MDA-MB-231 cells.

We then measured the time course of cortactin tyrosine phosphorylation in invadopodia following EGF stimulation. Cortactin phosphorylation in invadopodium precursors was measured using phosphospecific antibodies that specifically recognize cortactin that is tyrosine phosphorylated at tyrosines 421 or 466 in cells expressing cortactin WT–TagRFP at various times after EGF stimulation. Consistent with the actin barbed end data described above, cortactin phosphorylation of tyrosine 421 and 466 was increased three minutes after EGF stimulation at invadopodium precursors (supplementary material Fig. S2A–D). Together, these data demonstrate that phosphorylation of both tyrosines 421 and 466, but not tyrosine 482, is required for EGF-dependent generation of free actin barbed ends at invadopodium precursors.

Cortactin phosphorylation of tyrosines 421 and 466, but not 482, regulates Nck1 recruitment to invadopodia

Cortactin phosphorylation recruits the N-WASp activator, Nck1, to invadopodia (Oser et al., 2009). However, it is unclear which specific phosphorylation site mediates Nck1 recruitment and activation at invadopodia. Nck1 colocalization with cortactin at mature matrix-degrading invadopodia was analyzed using Pearson's correlation analysis. Compared with cells expressing cortactin WT–TagRFP, Nck1–cortactin colocalization at matrix-degrading invadopodia was significantly reduced in cells expressing cortactin Y3F–TagRFP (Fig. 2A,B). These data confirm the importance of cortactin phosphorylation for Nck1 recruitment to invadopodia in MDA-MB-231 cells, as previously shown in MTLn3 cells (Oser et al., 2009). In parallel with the requirement of tyrosines 421 and 466 for EGF-induced actin barbed end generation, the phosphorylation of tyrosines 421 and 466, but not 482, is important for Nck1–cortactin colocalization at invadopodia (Fig. 2A,B). Together, these results suggest that cortactin tyrosine phosphorylation of residues 421 and 466 promotes Nck1-recruitment to invadopodia to stimulate formation of actin barbed ends for actin polymerization.

Nck1 binds to cortactin phosphorylated on either tyrosine 421 or 466 in vitro

To determine whether Nck1 has a specificity for one of the cortactin phosphorylation sites in vitro, we performed in vitro pull-down assays to determine relative binding affinities using purified Nck1 and purified cortactin that was either unphosphorylated, phosphorylated on all three sites (WT CortP), phosphorylated on both tyrosines 421 and 466 (Cort421Y,466Y), or phosphorylated

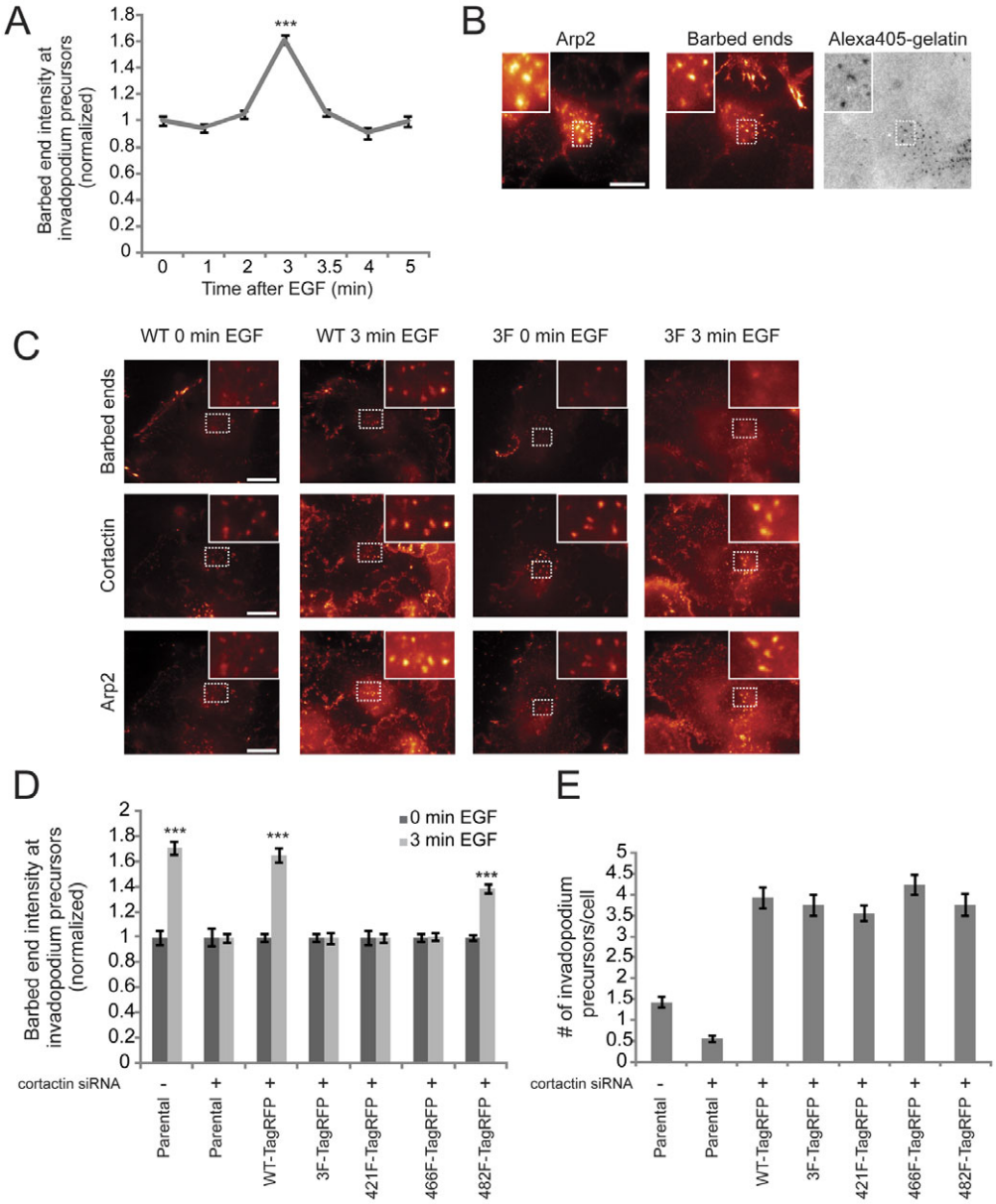

Fig. 1. Cortactin phosphorylation of tyrosines 421 and 466, but not 482, is required for actin polymerization in invadopodia. (**A**) Quantification of actin barbed end intensity at invadopodium precursors at times indicated after EGF stimulation normalized to 0 minutes EGF. Each experiment was repeated at least three times; the number of invadopodium precursors is given in brackets: 0 (652), 1 (601), 2 (727), 3(753), 3.5 (478), 4 (447) and 5 minutes (509). (**B**) Representative image of MDA-MB-231 cells plated on Alexa Fluor 405–gelatin matrix stained for barbed ends and Arp2 showing that new actin barbed ends are enriched in mature invadopodia that are actively degrading matrix (arrowheads). (**C**) Representative images of actin barbed ends, cortactin–TagRFP, and Arp2 at invadopodium precursors at 0 and 3 minutes in response to EGF in cells expressing cortactin WT–TagRFP or Y3F–TagRFP. (**D**) Quantification of barbed end intensity at invadopodium precursors in parental MDA-MB-231 cells or in cells expressing cortactin–TagRFP tyrosine phosphorylation mutants treated with cortactin siRNA to knockdown endogenous cortactin normalized to 0 minutes EGF. Each experiment was repeated three times. The number of invadopodium precursors is given in brackets: parental– 0 (80) and 3 minutes (130); parental+ 0 (47) and 3 minutes (110); WT+ 0 (256) and 3 minutes (167); Y3F+ 0 (221) and 3 minutes (223); Y421F+ 0 (108) and 3 minutes (197); Y466F+ 0 (403) and 3 minutes (292); Y482F+ 0 (235) and 3 minutes (175); – indicates control siRNA, + indicates cortactin siRNA. (**E**) Quantification of the number of invadopodium precursors per cell (as described in Materials and Methods) in cells stably expressing the cortactin–TagRFP tyrosine phosphorylation mutants treated with cortactin siRNA to knockdown endogenous cortactin. The number of cells scored from three independent experiments is given in brackets: parental– (200), parental+ (200), WT+ (200), Y3F+ (158), Y421F+ (173), Y466F + (126), Y482F+ (103). For all *P* values, results are compared with 0 minutes for each sample. Insets show close ups of invadopodium precursors. Scale bars: 10 μm.

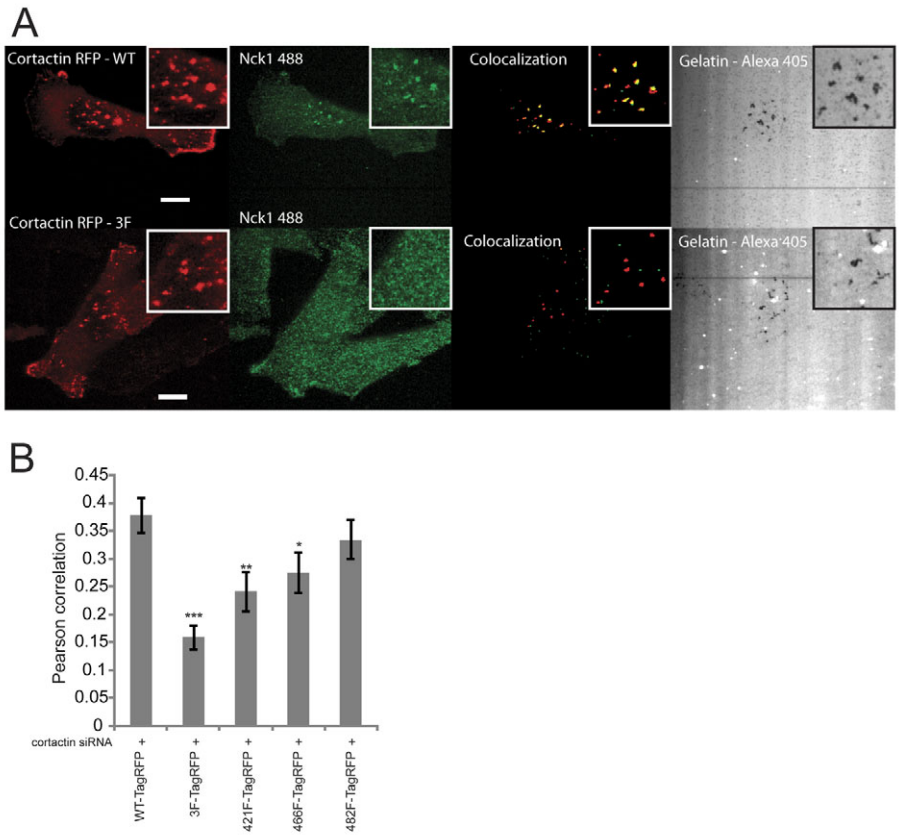

Fig. 2. Cortactin phosphorylation of tyrosines 421 and 466, but not 482, regulates Nck1 recruitment to invadopodia. (**A**) Representative images of cells expressing cortactin WT–TagRFP or Y3F–TagRFP plated on Alexa Fluor 405–gelatin matrix fixed and stained for cortactin and Nck1 showing that cells expressing cortactin WT–TagRFP, but not Y3F–TagRFP show colocalization of cortactin and Nck1 at invadopodia that are actively degrading matrix (insets). Scale bars: 10 µm. (**B**) Quantification of Pearson's correlation between cortactin and Nck1 at matrix-degrading invadopodia as described in Materials and Methods in cells stably expressing cortactin–TagRFP tyrosine phosphorylation mutants treated with cortactin siRNA to knockdown endogenous cortactin. Number of fields scored from four independent experiments are given in brackets: WT (23), Y3F (26), Y421F (20), Y466F (20), Y482F (14). For *P* values, results are compared with WT–TagRFP.

only on either 421 (Cort 421Y) or 466 (Cort 466Y) (supplementary material Fig. S3). The results show that Nck1 binds to WT CortP with micromolar affinity (K_d=1.86±0.66 µM), but does not bind to unphosphorylated cortactin, demonstrating that the Nck1–cortactin binding interaction is mediated by cortactin tyrosine phosphorylation (Fig. 3A). Furthermore, Nck1 binds to cortactin phosphorylated on tyrosine 466 with a similar K_d (K_d=3.0±1.53 µM) to that measured for WT CortP. Interestingly, Nck1 binds with twofold higher affinity to cortactin phosphorylated on tyrosine 466 (K_d=3.0±1.53 µM) compared with 421 (K_d=6.0±0.77 µM) (Fig. 3A,B), consistent with the slightly weaker binding of Nck1 to phosphorylated 421, 466 (K_d=3.90±0.48 µM). Taken together, these results suggest that Nck1 binds to phosphotyrosines 421 and 466 on cortactin, but with a modestly higher affinity for phosphotyrosine 466 over phosphotyrosine 421 in vitro.

Tyrosines 421 and 466 on cortactin are essential for the FRET interaction between cortactin and Nck1

To determine which cortactin phosphorylation sites are important for the Nck1–cortactin interaction in invadopodia, FRET acceptor photobleaching experiments were performed between cortactin (acceptor) and Nck1 (donor) using the cortactin–TagRFP phospho-mutant cell lines with endogenous cortactin knocked down (controls are described in detail in Materials and Methods and shown in supplementary material Fig. S4). FRET between cortactin and Nck1 in matrix-degrading invadopodia was analyzed. A significant FRET interaction (defined by the Rayleigh criterion as two proteins <8 nm apart) between Nck1–GFP and cortactin WT–TagRFP was observed (Fig. 4A,B, sensitized emission FRET control in supplementary material Fig. S4C,D), which was significantly inhibited in cells expressing cortactin Y3F–TagRFP, demonstrating that cortactin tyrosine phosphorylation is important for the Nck1–cortactin FRET interaction at invadopodia in MDA-MB-231 cells (Fig. 4A,B). Consistent with colocalization results described above (Fig. 2) and in vitro biochemistry (Fig. 3), FRET between Nck1 and cortactin was significantly reduced in cells expressing Y421F and Y466F, but not Y482F, suggesting that phosphorylation of both tyrosines 421 and 466, but not 482, is important for the Nck1–cortactin FRET interaction in matrix-degrading invadopodia (Fig. 4A,B).

To determine the specificity of individual phosphotyrosines 421 or 466 for mediating the FRET interaction between cortactin and Nck1, FRET between cortactin and Nck1 was analyzed in cortactin–TagRFP cell lines expressing Y466F/Y482F or Y421F/Y482F. Interestingly, cells expressing cortactin Y421F/Y482F–TagRFP, in which cortactin tyrosine 466 is the only available phosphorylation site, exhibited a significantly higher FRET interaction with Nck1 compared with cells expressing cortactin Y466F/Y482F–TagRFP, where tyrosine 421 on cortactin is the only available tyrosine phosphorylation site (Fig. 4C). This suggests that Nck1 might interact preferentially with phosphorylated tyrosine 466 compared with tyrosine 421 in invadopodia.

A recent study concluded that tyrosine phosphorylation of Tks5 recruits Nck1 to invadopodia in melanoma cells (Stylli et al., 2009). To ensure that cortactin–Nck1 interactions can occur in MDA-MB-231 cells independently of Tks5, immunoprecipitation experiments were performed between cortactin and Nck1 in cells stimulated with pervanadate or EGF when Tks5 was knocked down via siRNA (supplementary material Fig. S5). Nck1 co-immunoprecipitated with cortactin even when Tks5 levels were significantly reduced (supplementary material Fig. S5B–E). It is important to note that these experiments interrogate Nck1–cortactin

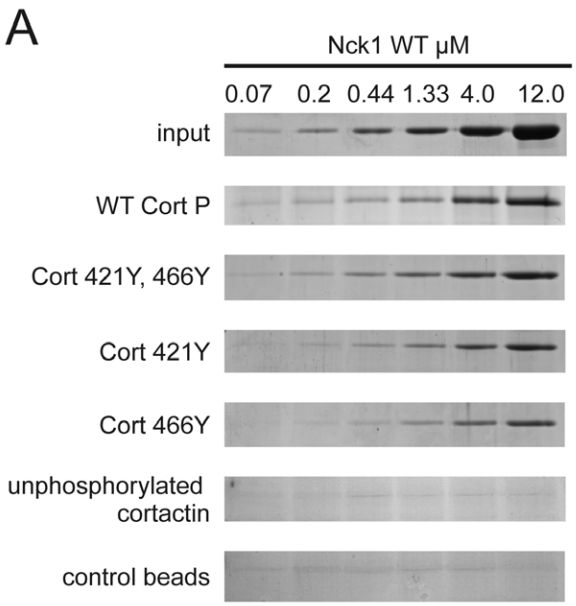

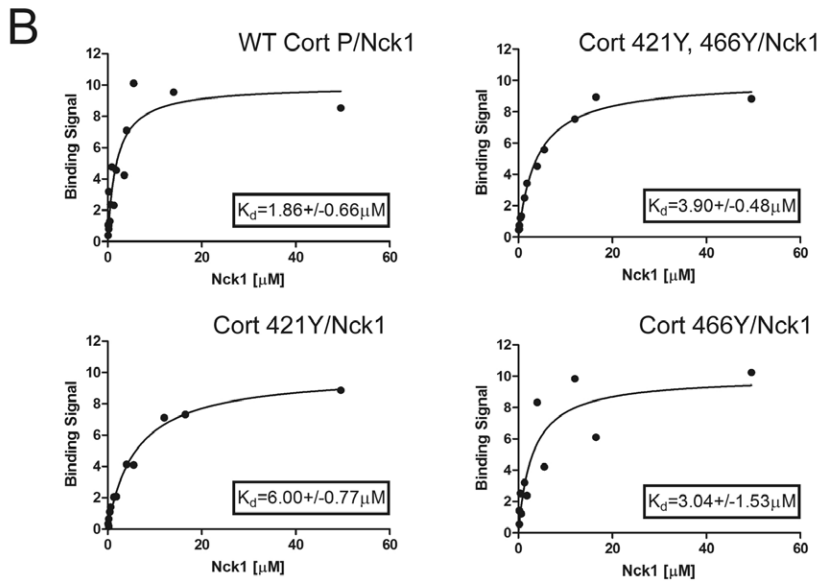

Fig. 3. Nck1 binds to cortactin phosphorylated tyrosines 421 or 466. In vitro pull-down assays (as described in Materials and Methods) were perform using purified Nck1 and purified cortactin that was either unphosphorylated, phosphorylated on all three sites (WT CortP), phosphorylated on both tyrosines 421 and 466 (Cort421Y,466Y), or phosphorylated only on either tyrosine 421 (Cort 421Y) or 466 (Cort 466Y). (**A**) Coomassie-stained gels and (**B**) quantification of the binding signal of Nck1 to WT CortP; Cort421Y,466Y; Cort 421Y; or Cort 466Y from in vitro pull-down assays at increasing concentrations of Nck1. Number of data points for calculation of the dissociation constant (K_d) are given in brackets: WT CortP (15), Cort 421Y,466Y (12), Cort 421Y (12), Cort 466Y (11). No binding of Nck1 to unphosphorylated cortactin was observed.

interaction in the context of the whole cell lysate and not specifically at invadopodia. These results suggest that cortactin can bind to Nck1 in MDA-MB-231 cells independently of Tks5.

Nck1 requires its SH2 domain to localize to and stimulate actin polymerization within invadopodia

The Nck1 SH2 domain binds phosphorylated cortactin in vitro (Lapetina et al., 2009). Therefore, we hypothesized that the SH2 domain mediates Nck1 recruitment to invadopodia by binding phosphorylated cortactin. To test this, endogenous Nck1 was transiently knocked down in MDA-MB-231 and cells were rescued by transient transfection of GFP, Nck1 WT–GFP, or a Nck1 mutant bearing a binding defective mutation in the SH2 domain (R308K–GFP) which prevents binding to phosphotyrosine-containing proteins (Fig. 5A). The knockdown was specific for Nck1 as it did not alter protein expression levels of Nck2 in MDA-MB-231 cells (supplementary material Fig. S3B). The results clearly show that Nck1 localizes with cortactin to matrix-degrading invadopodia in cells expressing Nck1 WT–GFP, but not Nck1 R308K–GFP (Fig. 5C,D), demonstrating that an intact and functional Nck1 SH2 domain is required for its localization to invadopodia.

Based on our results, we hypothesize that recruitment of Nck1 by cortactin phosphorylation is crucial for F-actin barbed end generation in invadopodia. To test whether the Nck1 SH2 domain is required for barbed end formation at invadopodium precursors, the barbed end assay was performed using cells expressing GFP, Nck1 WT–GFP, or Nck1 R308K–GFP, with Nck1 transiently knocked down. The results indicate that Nck1 is important for barbed end formation at invadopodium precursors formed in response to EGF (Fig. 5E). Furthermore, Nck1 WT–GFP, but not Nck1 R308K–GFP, was able to rescue new actin barbed end generation in response to EGF, suggesting that the Nck1 SH2 domain is important for the generation of free barbed ends in invadopodium precursors (Fig. 5E).

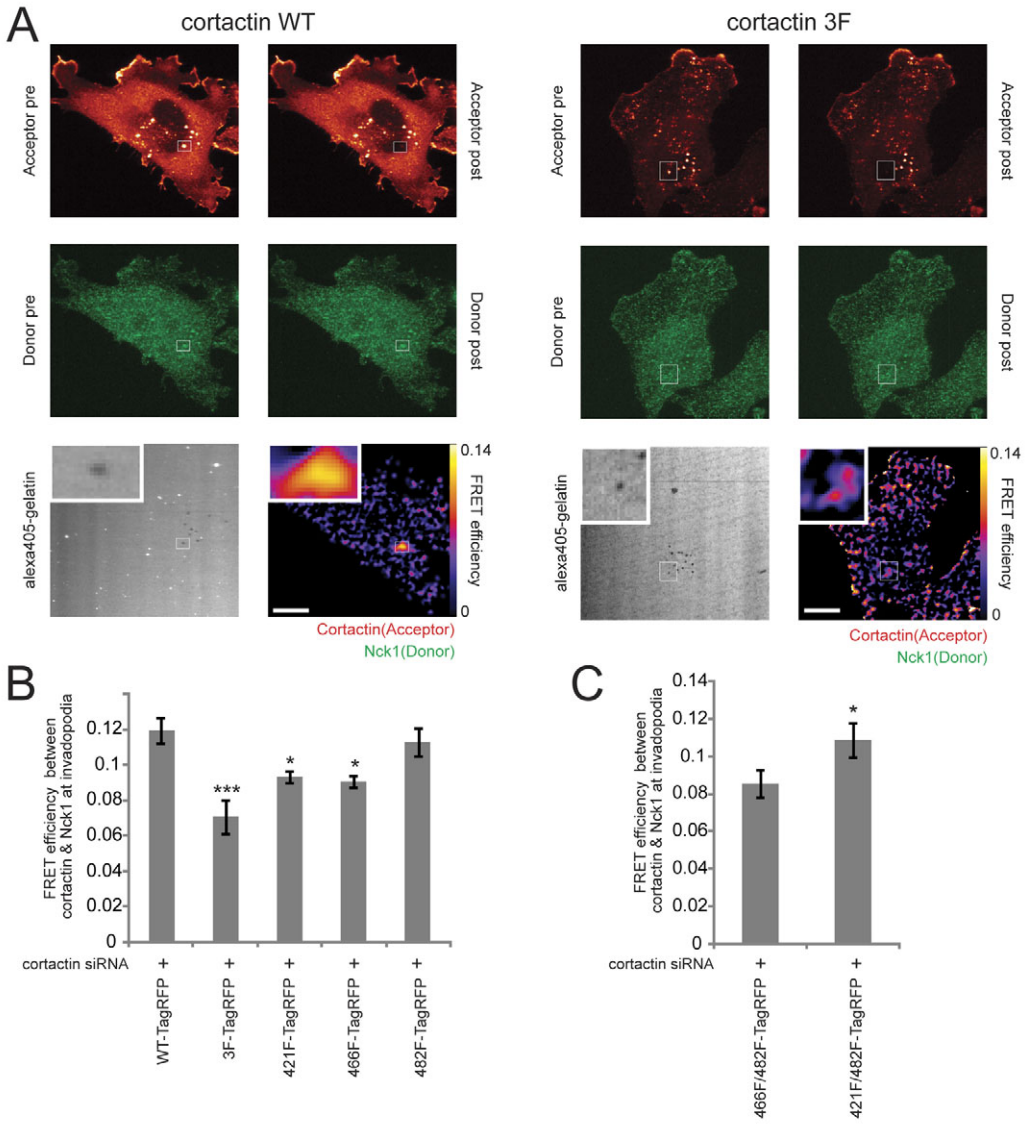

Fig. 4. Nck1 interacts with cortactin on tyrosines 421 and 466 in invadopodia, with a slight preference for tyrosine 466. (**A**) Representative FRET efficiency images between cortactin and Nck1 in matrix-degrading invadopodia in cells expressing cortactin WT–TagRFP or Y3F–TagRFP; cortactin (red), Nck1 (green); box indicates bleached area. Top left inset shows close up of FRET efficiency between cortactin and Nck1 at matrix-degrading invadopodia. Scale bars: 10 µm. (**B**,**C**) Quantification of FRET between cortactin and Nck1 at matrix-degrading invadopodia in cells expressing cortactin–TagRFP tyrosine phosphorylation mutants treated with cortactin siRNA to knockdown endogenous cortactin. For *P* values, results are compared with cortactin WT–TagRFP in B. Four independent experiments were performed.

We tested whether the interaction between cortactin and Nck1 was important for ECM degradation activity by invadopodia using an invadopodium degradation assay (Artym et al., 2009; Oser et al., 2009). The results show that degradation activity in cells expressing Nck1 R308K–GFP is significantly reduced compared with cells expressing Nck1 WT–GFP (Fig. 5F), demonstrating that formation of matrix-degrading invadopodia in cells expressing Nck1 R308K–GFP (as shown in Fig. 5C) is a rare event. Furthermore, degradation activity in cells expressing the cortactin Y3F–TagRFP mutant was also reduced compared with cells expressing cortactin WT–TagRFP (Fig. 5G). In summary, our results suggest that the interaction between cortactin phosphotyrosines 421 and 466 and the Nck1 SH2 domain mediates Nck1 recruitment to invadopodia (Figs 2, 5), which mediates subsequent actin polymerization in invadopodia (Figs 1, 5) and matrix degradation activity at these sites (Fig. 5F,G).

Cortactin phosphorylation of tyrosines 421 and 466, but not 482, is important for proteolysis-dependent tumor cell invasion

Generation of free barbed ends and actin polymerization is required for maturation to a degradation-competent invadopodium (Oser et al., 2009). Therefore, we hypothesized that the cortactin phosphorylation site mutants that were unable to generate free barbed ends in invadopodia would exhibit significant defects in their ability to invade through Matrigel that requires matrix proteolysis for invasion. To test this, Matrigel invasion assays were performed in the presence or absence of GM6001, a broad spectrum MMP inhibitor, using cortactin–TagRFP mutant cell lines with endogenous cortactin knocked down. The MMP inhibitor dramatically blocked invasion through Matrigel (Fig. 6A) demonstrating that matrix proteolysis is required for invasion in this assay, as previously reported (Chan et al., 2009). Compared with control cells, invasion was strongly inhibited in cortactin knockdown cells (Fig. 6B), demonstrating that cortactin is crucial for proteolysis-dependent tumor cell invasion. Furthermore, compared with cells expressing cortactin WT–TagRFP, invasion was dramatically inhibited in cells expressing cortactin Y3F–TagRFP (Fig. 6C), showing that tyrosine phosphorylation of cortactin is required for invasion through Matrigel. Invasion was also completely inhibited in cells expressing the Y466F cortactin mutant and only partially reduced in cells expressing the Y421F cortactin mutant, whereas the invasion of cells expressing the

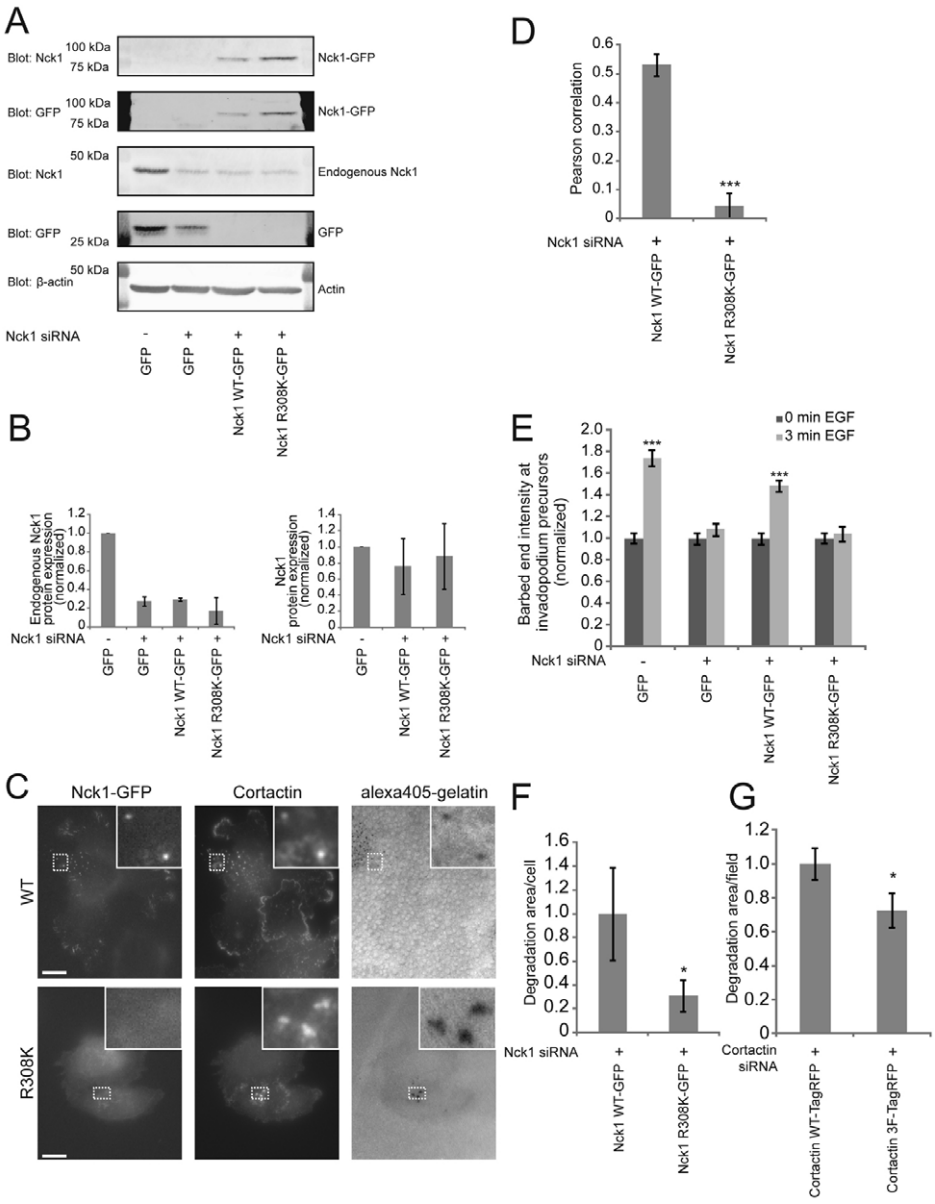

Fig. 5. The SH2 domain of Nck1 is required for Nck1 localization to invadopodia and actin polymerization in invadopodia. (**A**) Representative immunoblot and (**B**) quantification of knockdown (left) and overexpression (right) of whole cell lysates blotted for GFP, Nck1, and β-actin from MDA-MB-231 cells transiently expressing Nck1 WT–GFP or a phosphotyrosine binding defective SH2 domain mutant (R308K–GFP) treated with Nck1 siRNA to knockdown endogenous Nck1 72 hours prior to cell lysis. Three independent experiments. (**C**) Representative images of cells expressing Nck1 WT–GFP or Nck1 R308K–GFP mutant plated on Alexa Fluor 405–gelatin matrix, fixed, and stained for cortactin and Nck1, showing that cells expressing Nck1 WT–GFP, but not Nck1 R308K–GFP colocalize with cortactin in matrix-degrading invadopodia (insets). Scale bars: 10 μm. (**D**) Quantification of Pearson's correlation between Nck1 and cortactin at matrix-degrading invadopodia (as described in Materials and Methods) in cells expressing Nck1 WT–GFP or Nck1 R308K–GFP treated with Nck1 siRNA to knockdown endogenous cortactin. Number of fields scored from two independent experiments are given in brackets: WT (7), R308K (7). (**E**) Quantification of actin barbed end intensity in invadopodium precursors in cells expressing GFP, Nck1–GFP, or the Nck1 R308K–GFP mutant with endogenous Nck1 knocked down, normalized to 0 minutes EGF. Number of invadopodium precursors is given in brackets; three independent experiments: GFP– 0 (234) and 3 minutes (194); GFP+ 0 (203) and 3 minutes (280); WT+ 0 (185) and 3 minutes (276); R308K+ 0 (250) and 3 minutes (189). For *P* values, results are compared with 3 minute Nck1 knockdown cells expressing GFP; – indicates control siRNA, + indicates Nck1 siRNA. (**F**) Quantification of degradation area per cell in cells expressing either Nck1 WT–GFP or Nck1 R308K–GFP mutant with endogenous Nck1 knocked down, normalized to Nck1 WT–GFP. Number of GFP transfected cells are given in brackets; two independent experiments: Nck1 WT–GFP+ (13), Nck1 R308K–GFP+ (26); + indicates Nck1 siRNA. (**G**) Quantification of degradation area per field in cells expressing either cortactin WT–TagRFP or cortactin Y3F–TagRFP with endogenous cortactin knocked down, normalized to cortactin WT–TagRFP. Number of fields from five independent experiments are given in brackets: cortactin WT–TagRFP+ (53), cortactin Y3F–TagRFP+ (50); + indicates cortactin siRNA.

Y482F cortactin mutant was similar to WT (Fig. 6C). These phenotypes were not due to a gross defect in migration because all cortactin–TagRFP mutants were able to migrate through transwell filters in the absence of Matrigel at nearly identical rates (data not shown). Overall, the results indicate that phosphorylation of tyrosines 421 and 466, but not 482, are important for tumor cell

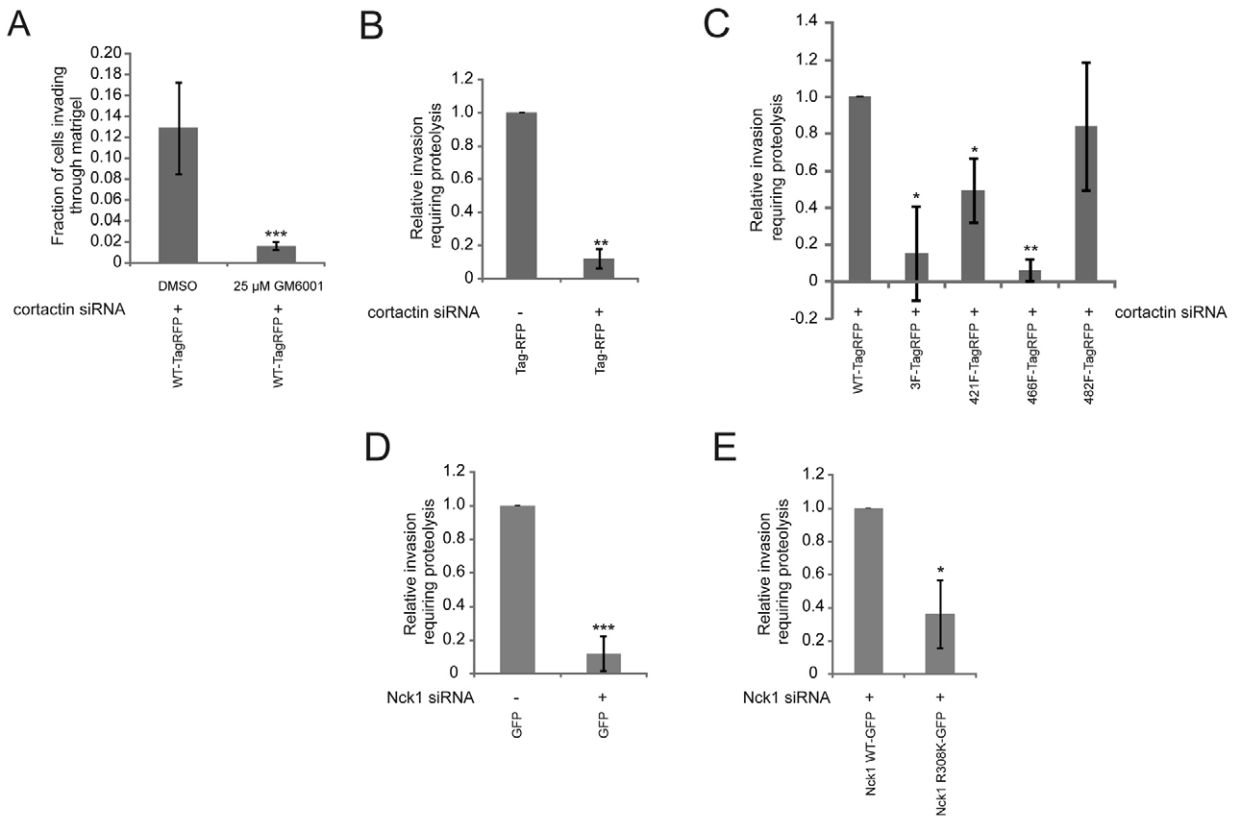

Fig. 6. Cortactin phosphorylation of tyrosines 421 and 466, but not 482, is important for proteolysis-dependent tumor cell invasion in vitro. (**A–E**) The transwell invasion assay was performed as described in Materials and Methods. (**A**) Quantification of fraction of cells invading through Matrigel in cortactin WT–TagRFP cells treated with DMSO or 25 µM GM6001. (**B**) Quantification of relative invasion through Matrigel requiring matrix proteolysis in cortactin knockdown cells normalized to controls siRNA. Three independent experiments. (**C**) Quantification of relative invasion through Matrigel requiring matrix proteolysis in cells stably expressing the cortactin–TagRFP tyrosine phosphorylation mutants treated with cortactin siRNA to knockdown endogenous cortactin. For *P* values, results are compared with RFP–WT; three independent experiments. (**D**) Quantification of relative invasion through Matrigel requiring matrix proteolysis in Nck1 knockdown cells expressing GFP normalized to control siRNA. Three independent experiments. (**E**) Quantification of relative invasion requiring matrix proteolysis in cells expressing Nck1 WT–GFP or Nck1 R308K–GFP transfected with Nck1 siRNA to knockdown endogenous Nck1. Three independent experiments.

invasion through Matrigel, and that 466 is the most crucial tyrosine phosphorylation site on cortactin for regulating proteolysis-dependent tumor cell invasion.

Finally, we tested whether the Nck1 SH2 domain was important for invasion through Matrigel using Nck1 knockdown cells expressing Nck1 WT–GFP, or Nck1 R308K–GFP. The results indicate that Nck1 is required for proteolysis-dependent tumor cell invasion (Fig. 6D). Moreover, compared with cells expressing Nck1 WT–GFP, invasion was inhibited in cells expressing Nck1 R308K–GFP (Fig. 6E), showing that the Nck1 SH2 domain is important for tumor cell invasion through Matrigel (Fig. 6E). Together, these results strongly suggest that the interaction between cortactin phosphotyrosine residues 421 and particularly 466 and the Nck1 SH2 domain is required for proteolysis-dependent tumor cell invasion through Matrigel.

Discussion

Tyrosine phosphorylation of cortactin is crucial for actin polymerization both in vitro (Tehrani et al., 2007) and in invadopodia (Oser et al., 2009), and for tumor cell metastasis in vivo (Li et al., 2001). Robust stimulation of actin polymerization is essential for the maturation of invadopodium precursors (Oser et al., 2009). Here, we investigated which specific cortactin tyrosine phosphorylation sites are crucial for regulating actin polymerization in invadopodia during the activation stage that follows invadopodium precursor formation (Oser et al., 2009). We demonstrate that phosphorylation of tyrosines 421 and 466, but not 482, is crucial for the generation of free actin barbed ends in invadopodia. Similarly, Nck1 recruitment to invadopodia requires phosphorylation of tyrosines 421 and 466, but not 482. Interestingly, Nck1 requires its SH2 domain to localize to invadopodia, where it interacts preferentially with phosphotyrosine 466 in invadopodia. Disruption of these interactions blocks Nck1 recruitment to invadopodia, as well as EGF-induced barbed end generation in invadopodia. Finally, in vitro invasion is inhibited in cells that are unable to phosphorylate cortactin on tyrosine 421 or 466. Together, our results provide evidence that the interaction between phosphotyrosines 421 and 466 on cortactin and the Nck1 SH2 domain is crucial for actin polymerization in invadopodia, leading to invadopodium maturation and ultimately tumor cell invasion.

Role of cortactin tyrosine phosphorylation in the regulation of actin polymerization in invadopodia

Previously, we have shown that cortactin tyrosine phosphorylation is a crucial mediator of adhesion-dependent cell edge protrusions through stimulation of actin polymerization at the cell edge in spreading fibroblasts (Lapetina et al., 2009). We show that cortactin phosphorylation also regulates actin barbed end generation in the

specialized protrusions of invadopodia in human MDA-MB-231 metastatic mammary carcinoma cells. Consistent with this role, integrity of the cortactin phosphorylation sites also regulates metastasis of these cells to bone in a mouse model of breast cancer metastasis (Li et al., 2001), demonstrating a physiological importance of cortactin tyrosine phosphorylation.

Cortactin can also be post-translationally modified through other mechanisms beside tyrosine phosphorylation, such as serine phosphorylation by Erk (Martinez-Quiles et al., 2004), and acetylation–deacetylation cycles (Zhang et al., 2007). Interestingly, although it was reported that serine phosphorylation of cortactin might promote actin polymerization in fibroblasts (Martinez-Quiles et al., 2004), this modification has little impact on the function of Src-induced invadopodium-like structures in 3T3 fibroblasts (Webb et al., 2007). Another study in melanoma cells demonstrated that cortactin serine phosphorylation is important for the matrix degradation activity of invadopodia (Ayala et al., 2008), but it is not yet clear how serine phosphorylation regulates invadopodium maturation. These conflicting results suggest that serine phosphorylation might differentially regulate invadopodium maturation in different cancer cell types. Given that cortactin acetylation–deacetylation has been implicated in regulating cortactin interactions with F-actin (Zhang et al., 2007), it is possible that these modifications might also contribute to the regulation of actin dynamics during invadopodium maturation and tumor cell invasion.

In this study, we demonstrated that tyrosine phosphorylation of sites 421 and 466, but not 482, is required for the generation of free barbed ends in invadopodia. Cortactin tyrosine phosphorylation initiates both cofilin and Arp2/3-dependent pathways, leading to the generation of barbed ends in invadopodia, and both cofilin and Arp2/3-dependent pathways are required for efficient actin polymerization in invadopodia (Oser et al., 2009). Previous studies have demonstrated that cortactin phosphorylation (Ayala et al., 2008; Oser et al., 2009), Nck1 (Oser et al., 2009; Stylli et al., 2009; Yamaguchi et al., 2005), N-WASp, and the Arp2/3 complex (Desmarais et al., 2009; Yamaguchi et al., 2005) all have important roles during invadopodium maturation. We have previously shown that efficient actin polymerization is not required for invadopodium precursor formation, and that N-WASp, Arp2, and some F-actin are recruited to invadopodium precursors prior to actin polymerization, independently of cortactin tyrosine phosphorylation (Oser et al., 2009). Interestingly, serine phosphorylation of cortactin facilitates direct binding between cortactin and N-WASp (Martinez-Quiles et al., 2004), suggesting a possible mechanism that regulates N-WASp recruitment to invadopodia. Our data strongly suggest that N-WASp activity in invadopodia is controlled by cortactin tyrosine phosphorylation via recruitment of Nck1 (Oser et al., 2009). Thus, it appears that there are distinct mechanisms that regulate N-WASp recruitment versus N-WASp activation in invadopodia. In this study, we provide evidence that the Nck1-dependent Arp2/3 activation is specifically regulated by cortactin phosphotyrosines 421 and 466. Interestingly, we show that Nck1 can bind to both phosphotyrosines 421 and 466 in vitro, but abolishment of either phosphorylation site in vivo inhibits the generation of free barbed ends in invadopodia. This suggests that cortactin phosphorylation regulates other proteins, apart from Nck1, that control actin polymerization within invadopodia. Cofilin is one likely target for regulation by phosphorylated cortactin because phosphorylated cortactin promoted cofilin-dependent actin severing activity in vitro (Oser et al., 2009). We hypothesize that in invadopodia, cofilin severing activity initially generates free barbed ends and that these barbed ends are amplified through dendritic nucleation by the Nck1–N-WASp–Arp2/3 complex. Thus, cortactin phosphorylation-dependent control of cofilin and the Arp2/3 complex function together to polymerize actin at invadopodia. Consistent with this, we observed that the abolishment of either phosphotyrosine 421 or 466 (or Nck1 knockdown) leads to near complete inhibition of actin polymerization in invadopodia, suggesting that both cofilin and Arp2/3 pathways, regulated by cortactin phosphorylation, function synergistically to polymerize actin in invadopodia (DesMarais et al., 2004; Ichetovkin et al., 2002; Oser et al., 2009).

Our data suggest that phosphotyrosine 466 on cortactin is the preferred site for the Nck1 FRET interaction with cortactin in invadopodia, leading to activation of a previously described Nck1–N-WASp–Arp2/3 pathway (Lapetina et al., 2009; Oser et al., 2009; Tehrani et al., 2007). Future studies will determine whether specificity exists between specific phosphotyrosines on cortactin and other SH2 domain- or non-SH2 domain-containing proteins to initiate pathways leading to actin polymerization. For example, both cofilin and dynamin II are important for regulating the actin cytoskeleton in invadopodia (Baldassarre et al., 2003; Oser et al., 2009), both bind directly to cortactin (McNiven et al., 2000; Oser et al., 2009), and their interaction with cortactin is regulated by cortactin tyrosine phosphorylation (Oser et al., 2009; Zhu et al., 2007). It will be interesting to determine whether phosphorylation of specific tyrosines on cortactin control its ability to regulate the activities of cofilin and dynamin II in invadopodia.

Cortactin tyrosine phosphorylation is crucial for Nck1 recruitment to invadopodia

We provide evidence that cortactin tyrosine phosphorylation is crucial for Nck1 recruitment to invadopodia and that purified tyrosine phosphorylated cortactin directly binds to purified Nck1 in vitro, as previously reported (Tehrani et al., 2007). It was recently demonstrated in melanoma cells that Tks5 phosphorylation by Src is important for Nck1 recruitment to invadopodia (Stylli et al., 2009), although Tks5 was co-purified with other associated proteins (including cortactin) and direct binding between purified Nck1 and purified tyrosine phosphorylated Tks5 was not demonstrated. Previous studies have demonstrated that Tks5 recruits cortactin to podosomes in smooth muscle cells (Crimaldi et al., 2009). Here, we show that the cortactin–Nck1 interaction in MDA-MB-231 cells is independent of Tks5. Together, these results suggest that Nck1 recruitment to invadopodia is mediated by a direct binding interaction between cortactin and Nck1, and that Tks5 might have an indirect role in Nck1 recruitment to invadopodia in MDA-MB-231 cells. Future studies will be required to determine the specificity of Nck1 for other phosphotyrosine-containing proteins in invadopodia.

Specificity of SH2 domain-containing proteins for phosphorylated cortactin

Recent studies on HS1, the hematopoetic homolog of cortactin, have demonstrated that specific tyrosine phosphorylation sites have distinct roles in chemotaxis (Y378) and synapse formation, cytolysis, and adhesion (Y397) in natural killer cells, and immunological synapse formation in T cells (Butler et al., 2008; Gomez et al., 2006). Specifically, phosphorylation of tyrosine 397, but not 378, is crucial for the localization and activation of Vav1, a GEF that activates Rac and Cdc42, at the lytic synapse in natural

killer cells (Butler et al., 2008) and the immunological synapse in T cells (Gomez et al., 2006). Here, we show that phosphorylation of cortactin tyrosines 421 and 466 are the crucial sites that regulate actin barbed end formation, and that the FRET interaction between cortactin and Nck1 might preferentially occur downstream of phosphotyrosine 466. Interestingly, GST-fusions of the SH2 domain of Nck1, but not Nck2, binds to phosphorylated cortactin in vitro (C.C.M., unpublished data) demonstrating a specific interaction between phosphorylated cortactin and Nck1. Consistent with this observation, we show that Nck2 is unable to compensate for Nck1 function during invadopodium maturation. Together, these studies provide evidence that distinct signaling pathways are activated downstream of tyrosine phosphorylation of specific sites on cortactin and HS1. Invadopodia are enriched in phosphotyrosine-containing proteins, and the presence of phosphotyrosines is highly correlated with the matrix degradation activity of invadopodia (Bowden et al., 2006). Future studies will be aimed at investigating the specificity between phosphotyrosines and SH2 domain-containing proteins in invadopodia to elucidate our understanding of the molecular mechanisms that regulate invadopodium maturation.

Materials and Methods

Antibodies

For immunofluorescence, cortactin (ab-33333) and Nck1 (ab-14588) were from Abcam; Arp2 (sc-H-84) and Tks5 (sc-30122) were from Santa Cruz Biotechnology; pY421 and pY466 were from Sigma, and anti-biotin FITC was from Jackson. Alexa Fluor-conjugated secondary antibodies were from Invitrogen. For immunoprecipitation, cortactin 4F11 was from Upstate. For immunoblots, cortactin (ab-33333) and Nck1 (11D10) were from Abcam; tRFP was from Evrogen; anti-β-actin (AC15) and pY421 were from Sigma and Biosource; pY466 was from Biosource; Nck1 (15B9) was from Cell Signaling; Nck2 (07-100) was from Upstate; and Nck1 (sc-56447), Tks5 (sc-30122) and HSP70 (sc32239) were from Santa Cruz Biotechnology. All immunoblot secondary antibodies were from Li-Cor (ms-680 and rb-800).

Cell culture and EGF and pervanadate stimulation

For all experiments, MDA-MB-231 cells were cultured in 10% FBS/DMEM with antibiotics. For barbed end and EGF stimulation experiments, cells plated on FN/gelatin matrix were starved in 0.5% FBS/0.8% BSA/DMEM for 12–16 hours and then stimulated with 2.5 nM EGF (Invitrogen #13247-051). For pervanadate stimulation experiments, cortactin–TagRFP cell lines were stimulated with 12 μM pervanadate 30 minutes prior to lysis as described previously (Cory et al., 2002).

Invadopodium degradation assay and immunofluorescence

The barbed end, invadopodium precursor formation, and EGF stimulation experiments were performed using MDA-MB-231 cells cultured on FN/gelatin matrix. For all cortactin cell line experiments, endogenous cortactin was knocked down 72–96 hours prior to the start of the experiment and confirmed by immunoblot. For all Nck1 cell line experiments, endogenous Nck1 was knocked down 72 hours prior to the start of the experiment and confirmed by immunoblot. FN/gelatin matrix was prepared as described previously (Chen, 1989). Briefly, MatTek dishes were treated with 2.5% gelatin/2.5% sucrose, crosslinked with 0.5% glutaraldehyde, treated with 10 μg/ml of unlabeled FN (Sigma), and then with 1 mg/ml $NaBH_4$ in PBS. The cells were fixed in 3.7% PFA and immunofluorescence was performed as described previously (Yamaguchi et al., 2005). For cortactin–Nck1 colocalization, degradation and FRET experiments, 100,000 MDA-MB-231 cells were plated on Alexa Fluor 405-labeled thin gelatin matrix 4 hours prior to fixation and the cells fixed in 3.7% PFA as described above. Alexa Fluor 405 (Invitrogen-A30000) was conjugated to gelatin (Sigma, G2500) as described previously (Artym et al., 2009) and thin matrix Alexa Fluor 405–gelatin matrix was prepared as previously described (Artym et al., 2006). Degradation area was quantified as described previously (Oser et al., 2009). For Fig. 5F, the degradation area per cell transfected with GFP was quantified, and for Fig. 5G, the degradation area per field was quantified. Cortactin WT–TagRFP rescued degradation in cortactin knockdown cells, verifying that the rescue constructs are functional (supplementary material Fig. S1E).

Barbed end assay

The barbed end assay was performed with MDA-MB-231 cells using biotin–actin as described previously (Oser et al., 2009). Briefly, cortactin–TagRFP cells lines, in which endogenous cortactin was transiently knocked down using siRNA, were starved, stimulated with EGF as described above, permeabilized with a permeabilization buffer (20 mM HEPES pH 7.5, 138 mM KCl, 4 mM $MgCl_2$, 3 mM EGTA, 0.2 mg/ml saponin, 1 mM ATP, 1% BSA) containing 0.4 μM biotin–actin (Cytoskeleton) for 1 minute at 37°C. Cells were fixed in 3.7% formaldehyde for 5 minutes, blocked in PBS containing 1% FBS, 1% BSA and 3 μM phalloidin, then stained with FITC anti-biotin to visualize barbed ends, and Arp2 to identify invadopodium precursors. The barbed end intensity at invadopodium precursors was quantified as mean gray value (mgv) at invadopodium precursors minus mgv of the background. The data was normalized to the control condition for each experiment. The difference in EGF-induced barbed end peaks is cell-type-specific (MDA-MB-231, 3 minutes; MTLn3, 1 minute) (Oser et al., 2009).

Cortactin–Nck1 FRET acceptor photobleaching

Cortactin–TagRFP cells lines in which endogenous cortactin was transiently knocked down using siRNA, were plated on Alexa Fluor 405-labeled gelatin for 4 hours and fixed using 3.7% PFA as described above. Immunofluorescence was performed using Nck1 (ab-14588), Alexa Fluor 488-labeled donkey anti-rabbit (donor) and cortactin (ab-33333), Alexa Fluor 555-labeled goat anti-mouse (acceptor) for the Nck1–cortactin experiments. For all fixed cell acceptor photobleaching FRET and immunofluorescence experiments, samples were stored in PBS and imaged the following day after fixation. Invadopodia were selected for FRET analysis that contained colocalized cortactin, Nck1 and matrix degradation, using the same criteria described below for cortactin–Nck1 colocalization analysis. Images were analyzed and FRET efficiency was calculated as E=1–(Donor pre/Donor post). All images were corrected for laser fluctuations, overall sample bleaching and background. Controls are shown in supplementary material Fig. S4. Included are controls for photoconversion, laser fluctuation and nonspecific molecular interactions. For microscopy set-up, including laser lines and filter settings, see Microscopy section in Materials and Methods.

Cortactin–Nck1 sensitized emission FRET

MDA-MB-231 cells expressing Nck1 WT–GFP and cortactin WT–TagRFP were subjected to live sensitized emission imaging as described previously (Feige et al., 2005). Cells expressing fluorescent constructs were imaged on an Olympus IX70 microscope with 60× NA 1.4 objectives and a Sensicam QE CCD. FRET images. Bleed-trough calculations were analyzed using PixFRET 1.5.0. Results are shown as FRET/Donor.

Cortactin–Nck1 colocalization analysis

Cortactin–TagRFP cells lines in which endogenous cortactin was transiently knocked down using siRNA, were plated on Alexa Fluor 405-labeled gelatin for 4 hours, fixed using 3.7% PFA, and immunostained for cortactin (ab-33333) and Nck1 (ab-14588). For Nck1–GFP experiments, GFP, Nck1 WT–GFP or Nck1 R308K–GFP were transiently transfected into MDA-MB-231 cells knocked down for endogenous Nck1. Cells were treated as described above and immunostained for cortactin (ab-33333). Images were processed using ImageJ Spot enhancing filter 2D (3.0 pixel Gaussian filter) and threshold levels set to select only invadopodia (entropy threshold). Invadopodia masks were generated using particle analysis tools. Based on the filters used to determine colocalization, the analysis does not measure the abundance of proteins at invadopodia, but simply the presence or absence of cortactin and Nck1 in the same structure. The images were then analyzed for colocalization (Pearson correlation, overlap and M1/M2) using the Jacop colocalization plugin for ImageJ. By using this technique, the colocalization analysis is restricted to real points of interest (invadopodia), which drastically reduces the presence of false positive correlation areas. This results in lower overall correlation, but in very high accuracy.

RNAi

Control nonsilencing siRNA was from Qiagen. Human-specific cortactin siGenome Smart Pool (M010508-00-0005), Nck1 siRNA (J-006354-06-0005) and Tks5 siGenome Smart Pool (M-006657-02-0005) were from Dharmacon. About 1×10^6 MDA-MB-231 cells were transfected with 2 μM siRNA using the Lonza Nucleofection Kit V protocol 72–96 hours prior to each experiment. Immunoblot analysis was used to confirm the knockdown for each experiment.

Constructs and cell lines

Murine cortactin and cortactin Y3F mutants were cloned as described previously (Lapetina et al., 2009). Single-site phosphorylation mutants of cortactin were generated via PCR mutagenesis, cloned into N1–TagRFP (Clontech Laboratories), and subcloned into the retroviral expression vector pLXSN (BD Biosciences). Amphotrophic Pheonix cells were transfected with Lipofectamine 2000. Retroviral sups were used to infect MDA-MB-231 cells, which were then selected with 600 μg/ml Geneticin. Expression levels of retrovirally expressed cortactin or cortactin mutants were determined by immunoblotting, and the signal was compared with endogenous cortactin in cells expressing empty TagRFP control vector. RNAi-resistant Nck1 and Nck1 SH2 mutant (R308K) were generated via PCR-based mutagenesis. Human Nck1 was cloned into pQC vectors and transiently transfected into MDA-MB-231 cells using the Lonza Nucleofection Kit V protocol 24 hours before each experiment.

Immunoprecipitation

Immunoprecipitation experiments were performed as described previously (Oser et al., 2009). Briefly, 1×10^6 MDA-MB-231 cells were plated on plastic tissue culture dishes 16 hours before the experiment. For the cortactin immunoprecipitation experiments described in supplementary material Fig. S5, the cells were stimulated with 12 μM pervanadate 30 minutes prior to cell lysis as described previously (Cory et al., 2002) or for 3 minutes with 5 nM EGF. After pervanadate or EGF stimulation, the cells were washed with cold PBS, and lysed in buffer containing 10 mM HEPES, 50 mM NaCl, 5 mM EGTA,.5 mM $MgCl_2$, 1% Triton X-100 and phosphatase (NaF and $NaVO_4$) and protease inhibitors. The lysates were centrifuged at 18,000 ***g*** for 10 minutes at 4°C and pre-cleaned with protein A/G agarose beads (sc-2003) for 30 minutes. The immunoprecipitate was rotated overnight with 2 μg cortactin antibody 4F11 or 2 μg control IgG1 antibody conjugated to protein A/G agarose beads. The immunoprecipitates were washed three times in lysis buffer and analyzed by immunoblot analysis. For quantification, control antibody immunoprecipitate mgv or co-immunoprecipitate mgv was subtracted from immunoprecipitate mgv or co-immunoprecipitate mgv. All values were corrected for area. The co-immunoprecipitates were normalized to the immunoprecipitate for each sample and then normalized to control siRNA.

Immunoblot analysis

For protein immunoblot analysis, whole cell lysates were prepared by washing twice with cold PBS before direct extraction in SDS-PAGE sample buffer. The samples were resolved by SDS-PAGE, transferred to nitrocellulose, blocked in Odyssey Blocking Solution (LiCor), incubated with primary antibodies, secondary antibodies, and then analyzed using the Odyssey (Li-Cor). For quantification, the mgv of each sample minus background corrected for area was calculated.

Invadopodium precursor formation analysis

MDA-MB-231 cell lines stably expressing murine cortactin–TagRFP mutants were treated with human-specific cortactin siRNA to deplete endogenous cortactin. The cells were fixed, immunofluorescence was performed, and invadopodium precursors were identified as colocalized cortactin–TagRFP and F-actin punctate structures. Invadopodium precursor formation was scored as the number of invadopodium precursors per cell and as the percentage of cells with invadopodium precursors.

Immunofluorescence analysis of cortactin tyrosine phosphorylation in invadopodia

MDA-MB-231 cell lines stably expressing murine cortactin WT–TagRFP were plated on FN/gelatin matrix, starved and stimulated with EGF as described above, and then fixed and stained with cortactin phosphospecific antibodies (pY421 or pY466) specific for mouse. The intensity (mgv – background) of cortactin–TagRFP, pY421-cortactin or pY466-cortactin in invadopodia was quantified, and the pY421-cortactin/cortactin–TagRFP or pY466-cortactin/cortactin–TagRFP ratios were calculated as a measure of phosphorylated cortactin in invadopodia at various times after EGF stimulation. The data were normalized to resting cells (0 minutes EGF) as a measure of relative fold change in cortactin tyrosine phosphorylation in response to EGF in invadopodia. Phosphorylation of site Y482 was not tested as there are no phosphospecific antibodies to site Y482 available.

Transwell invasion assay

The bottom surfaces of 8.0 μm transwell supports (Costar) were coated with 10 μg/ml fibronectin for 1 hour and allowed to air dry. The upper surfaces of the supports were coated with 50 μl reduced growth factor Matrigel (2.5 μg/ml) for 1 hour at 37°C. Excess Matrigel was removed and both chambers allowed to equilibrate in DMEM at 37°C for 1 hour. After equilibration, the bottom chamber was filled with 1 ml of 10% FBS/DMEM. 50,000 cells were resuspended in 200 μl 0.5% FBS/DMEM and plated in the upper chamber. Where indicated, broad spectrum MMP inhibitor GM6001 (25 μM) was added to both chambers. As an additional control, cells were also plated in transwell membranes without Matrigel and allowed to invade for 24 hours followed by fixation in 3.7% PFA. Cells that did not invade were removed from the upper surface of the membranes using cotton swabs, while cells on the bottom surface were stained with DAPI. Proteolysis-dependent invasion was calculated by subtracting the relative invasion in the presence of 25 μM GM6001 from the relative invasion without the GM6001 inhibitor. Results are based on analysis of 10 fields (20×) in three independent experiments.

Microscopy

The fixed cell experiments were performed at 25°C in PBS on a wide-field Olympus IX81 electronically motorized microscope. Images were acquired with a Sensicam QE cooled CCD camera using IP Lab 4.0. The cortactin–Nck1 acceptor photobleaching FRET and cortactin–Nck1 colocalization analysis were performed on a Zeiss LSM 5 LIVE DuoScan laser scanning microscope, using a 561 nm laser to bleach and excite the acceptor and a 488 nm laser to excite the donor. The acceptor and donor emissions were collected using 550–615 nm and 495–525 nm band pass filters, respectively, with a CCD camera using LSM 5 Live Duoscan software. Sensitized emission FRET experiments were performed on an Olympus IX70 microscope with a Sensicam QE CCD. All imaging was done using 60× or 63× N.A. 1.4 oil objectives. All live cell experiments were imaged at 37°C in L15 media.

Protein purification

Recombinant murine cortactin and cortactin mutants were purified from insect cells as previously described (Lapetina et al., 2009). Human Nck1 was cloned into the pFastbac vector (Qiagen) and expressed via the Bac-to-Bac system according to the manufacturer's protocol. Nck1 was purified with the same purification protocol as described for cortactin.

Cortactin–Nck1 in vitro binding experiments

Recombinant cortactin protein was covalently coupled to AminoLink Beads (Thermo Scientific) (1 mg/ml gel bed; 16.3 μM) according to the manufacturer's protocol. Nck1 protein was serially diluted 1:3, 20 μl was saved as input sample, and 490 μl of each dilution was added to Eppendorf tubes containing 50 μl cortactin bead slurry or 50 μl blank bead slurry blocked with excess Tris buffer. The reaction was incubated at 4°C while rotating for 30 minutes. The supernatant was removed and beads were rapidly resuspended with 1 ml cold binding buffer (3.65× PBS). Bound material was recovered with 4× Laemmli sample buffer and analyzed on 10% SDS-PAGE gels, stained with Coomassie Blue R-250, and scanned using a BioRad densitometer. Intensity levels were auto-adjusted in Quantity One Software. Integrated density measurements of the band and equal background area were made. This background measurement was subtracted from band density measurement. Binding curves were generated using the standard one-site binding function of GraphPad Prism software. For representative gels, the Adobe Photoshop autolevels function was used and gels cropped to display interaction bands.

Statistical analysis

Statistical significance was calculated using the unpaired, two-tailed Students *t*-test. Values were considered statistically significant if $P<0.05$. For all figures, $*P<0.05$, $**P<0.01$ and $***P<0.001$. Error bars represent s.e.m. ANOVA tests were positive for all experiments that contained multiple samples.

We thank the Condeelis, Cox and Segall laboratories and Scott Weed for helpful discussions, and the Analytical Imaging Facility for technical help. This work was funded by CA150344, CA113395 (M.O., M.M., J.C.), NIHCA133346, NIHNS39475, and an award from the Elsa U. Pardee Foundation (A.J.K.) and an NSF Graduate Research Fellowship (C.C.M.). Deposited in PMC for release after 12 months.

Supplementary material available online at
http://jcs.biologists.org/cgi/content/full/123/21/3662/DC1

References

Artym, V. V., Zhang, Y., Seillier-Moiseiwitsch, F., Yamada, K. M. and Mueller, S. C. (2006). Dynamic interactions of cortactin and membrane type 1 matrix metalloproteinase at invadopodia: defining the stages of invadopodia formation and function. *Cancer Res.* **66**, 3034-3043.

Artym, V. V., Yamada, K. M. and Mueller, S. C. (2009). ECM degradation assays for analyzing local cell invasion. *Methods Mol. Biol.* **522**, 211-219.

Ayala, I., Baldassarre, M., Giacchetti, G., Caldieri, G., Tete, S., Luini, A. and Buccione, R. (2008). Multiple regulatory inputs converge on cortactin to control invadopodia biogenesis and extracellular matrix degradation. *J. Cell Sci.* **121**, 369-378.

Baldassarre, M., Pompeo, A., Beznoussenko, G., Castaldi, C., Cortellino, S., McNiven, M. A., Luini, A. and Buccione, R. (2003). Dynamin participates in focal extracellular matrix degradation by invasive cells. *Mol. Biol. Cell* **14**, 1074-1084.

Bowden, E. T., Onikoyi, E., Slack, R., Myoui, A., Yoneda, T., Yamada, K. M. and Mueller, S. C. (2006). Co-localization of cortactin and phosphotyrosine identifies active invadopodia in human breast cancer cells. *Exp. Cell Res.* **312**, 1240-1253.

Butler, B., Kastendieck, D. H. and Cooper, J. A. (2008). Differently phosphorylated forms of the cortactin homolog HS1 mediate distinct functions in natural killer cells. *Nat. Immunol.* **9**, 887-897.

Chan, A. Y., Raft, S., Bailly, M., Wyckoff, J. B., Segall, J. E. and Condeelis, J. S. (1998). EGF stimulates an increase in actin nucleation and filament number at the leading edge of the lamellipod in mammary adenocarcinoma cells. *J. Cell Sci.* **111**, 199-211.

Chan, K. T., Cortesio, C. L. and Huttenlocher, A. (2009). FAK alters invadopodia and focal adhesion composition and dynamics to regulate breast cancer invasion. *J. Cell Biol.* **185**, 357-370.

Chen, W. T. (1989). Proteolytic activity of specialized surface protrusions formed at rosette contact sites of transformed cells. *J. Exp. Zool.* **251**, 167-185.

Clark, E. S., Whigham, A. S., Yarbrough, W. G. and Weaver, A. M. (2007). Cortactin is an essential regulator of matrix metalloproteinase secretion and extracellular matrix degradation in invadopodia. *Cancer Res.* **67**, 4227-4235.

Condeelis, J. and Segall, J. E. (2003). Intravital imaging of cell movement in tumours. *Nat. Rev. Cancer* **3**, 921-930.

Cory, G. O., Garg, R., Cramer, R. and Ridley, A. J. (2002). Phosphorylation of tyrosine 291 enhances the ability of WASp to stimulate actin polymerization and filopodium formation. Wiskott-Aldrich Syndrome protein. *J. Biol. Chem.* **277**, 45115-45121.

Crimaldi, L., Courtneidge, S. A. and Gimona, M. (2009). Tks5 recruits AFAP-110, p190RhoGAP, and cortactin for podosome formation. *Exp. Cell Res.* **315**, 2581-2592.
DesMarais, V., Macaluso, F., Condeelis, J. and Bailly, M. (2004). Synergistic interaction between the Arp2/3 complex and cofilin drives stimulated lamellipod extension. *J. Cell Sci.* **117**, 3499-3510.
Desmarais, V., Yamaguchi, H., Oser, M., Soon, L., Mouneimne, G., Sarmiento, C., Eddy, R. and Condeelis, J. (2009). N-WASP and cortactin are involved in invadopodium-dependent chemotaxis to EGF in breast tumor cells. *Cell Motil. Cytoskeleton* **66**, 303-316.
Feige, J. N., Sage, D., Wahli, W., Desvergne, B. and Gelman, L. (2005). PixFRET, an ImageJ plug-in for FRET calculation that can accommodate variations in spectral bleed-throughs. *Microsc. Res. Tech.* **68**, 51-58.
Gomez, T. S., McCarney, S. D., Carrizosa, E., Labno, C. M., Comiskey, E. O., Nolz, J. C., Zhu, P., Freedman, B. D., Clark, M. R., Rawlings, D. J. et al. (2006). HS1 functions as an essential actin-regulatory adaptor protein at the immune synapse. *Immunity* **24**, 741-752.
Ichetovkin, I., Grant, W. and Condeelis, J. (2002). Cofilin produces newly polymerized actin filaments that are preferred for dendritic nucleation by the Arp2/3 complex. *Curr. Biol.* **12**, 79-84.
Lapetina, S., Mader, C. C., Machida, K., Mayer, B. J. and Koleske, A. J. (2009). Arg interacts with cortactin to promote adhesion-dependent cell edge protrusion. *J. Cell Biol.* **185**, 503-519.
Li, Y., Tondravi, M., Liu, J., Smith, E., Haudenschild, C. C., Kaczmarek, M. and Zhan, X. (2001). Cortactin potentiates bone metastasis of breast cancer cells. *Cancer Res.* **61**, 6906-6911.
Machida, K., Thompson, C. M., Dierck, K., Jablonowski, K., Karkkainen, S., Liu, B., Zhang, H., Nash, P. D., Newman, D. K., Nollau, P. et al. (2007). High-throughput phosphotyrosine profiling using SH2 domains. *Mol. Cell* **26**, 899-915.
Martinez-Quiles, N., Ho, H. Y., Kirschner, M. W., Ramesh, N. and Geha, R. S. (2004). Erk/Src phosphorylation of cortactin acts as a switch on-switch off mechanism that controls its ability to activate N-WASP. *Mol. Cell. Biol.* **24**, 5269-5280.
McNiven, M. A., Kim, L., Krueger, E. W., Orth, J. D., Cao, H. and Wong, T. W. (2000). Regulated interactions between dynamin and the actin-binding protein cortactin modulate cell shape. *J. Cell Biol.* **151**, 187-198.
Oser, M., Yamaguchi, H., Mader, C. C., Bravo-Cordero, J. J., Arias, M., Chen, X., Desmarais, V., van Rheenen, J., Koleske, A. J. and Condeelis, J. (2009). Cortactin regulates cofilin and N-WASp activities to control the stages of invadopodium assembly and maturation. *J. Cell Biol.* **186**, 571-587.
Poincloux, R., Lizarraga, F. and Chavrier, P. (2009). Matrix invasion by tumour cells: a focus on MT1-MMP trafficking to invadopodia. *J. Cell Sci.* **122**, 3015-3024.
Schoumacher, M., Goldman, R. D., Louvard, D. and Vignjevic, D. M. (2010). Actin, microtubules, and vimentin intermediate filaments cooperate for elongation of invadopodia. *J. Cell Biol.* **189**, 541-556.
Stylli, S. S., Stacey, T. T., Verhagen, A. M., Xu, S. S., Pass, I., Courtneidge, S. A. and Lock, P. (2009). Nck adaptor proteins link Tks5 to invadopodia actin regulation and ECM degradation. *J. Cell Sci.* **122**, 2727-2740.
Tehrani, S., Tomasevic, N., Weed, S., Sakowicz, R. and Cooper, J. A. (2007). Src phosphorylation of cortactin enhances actin assembly. *Proc. Natl. Acad. Sci. USA* **104**, 11933-11938.
Wang, W., Mouneimne, G., Sidani, M., Wyckoff, J., Chen, X., Makris, A., Goswami, S., Bresnick, A. R. and Condeelis, J. S. (2006). The activity status of cofilin is directly related to invasion, intravasation, and metastasis of mammary tumors. *J. Cell Biol.* **173**, 395-404.
Weaver, A. M. (2008). Cortactin in tumor invasiveness. *Cancer Lett.* **265**, 157-166.
Webb, B. A., Jia, L., Eves, R. and Mak, A. S. (2007). Dissecting the functional domain requirements of cortactin in invadopodia formation. *Eur. J. Cell Biol.* **86**, 189-206.
Yamaguchi, H., Lorenz, M., Kempiak, S., Sarmiento, C., Coniglio, S., Symons, M., Segall, J., Eddy, R., Miki, H., Takenawa, T. et al. (2005). Molecular mechanisms of invadopodium formation: the role of the N-WASP-Arp2/3 complex pathway and cofilin. *J. Cell Biol.* **168**, 441-452.
Zhang, X., Yuan, Z., Zhang, Y., Yong, S., Salas-Burgos, A., Koomen, J., Olashaw, N., Parsons, J. T., Yang, X. J., Dent, S. R. et al. (2007). HDAC6 modulates cell motility by altering the acetylation level of cortactin. *Mol. Cell* **27**, 197-213.
Zhu, J., Yu, D., Zeng, X. C., Zhou, K. and Zhan, X. (2007). Receptor-mediated endocytosis involves tyrosine phosphorylation of cortactin. *J. Biol. Chem.* **282**, 16086-16094.

Journal of Cell Science

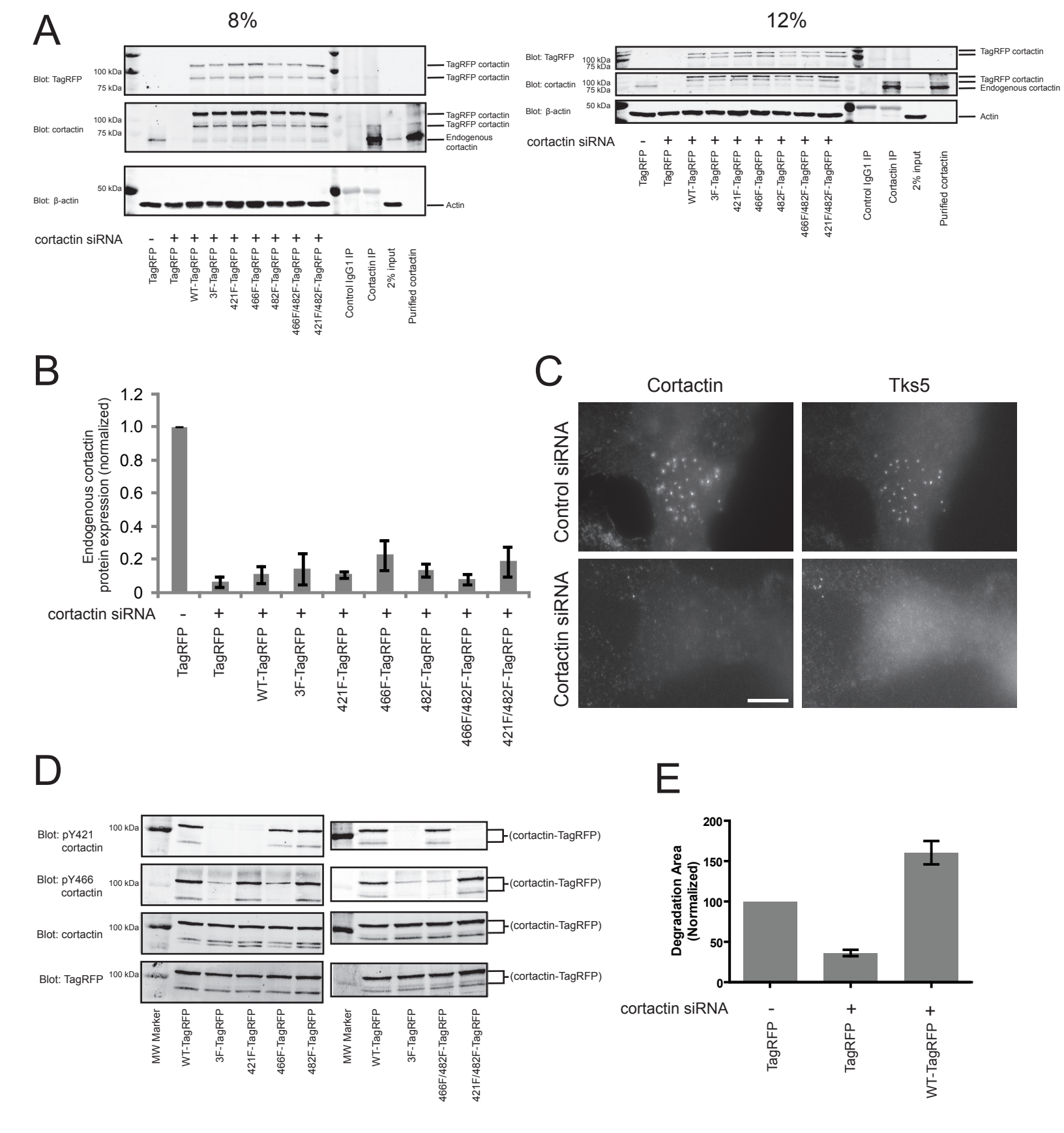
A
8%
12%
Blot: TagRFP
Blot: cortactin
Blot: β-actin
100 kDa
75 kDa
50 kDa
TagRFP cortactin
Endogenous cortactin
Actin
cortactin siRNA
TagRFP
WT-TagRFP
3F-TagRFP
421F-TagRFP
466F-TagRFP
482F-TagRFP
466F/482F-TagRFP
421F/482F-TagRFP
Control IgG1 IP
Cortactin IP
2% input
Purified cortactin
B
Endogenous cortactin protein expression (normalized)
C
Cortactin
Tks5
Control siRNA
Cortactin siRNA
D
Blot: pY421 cortactin
Blot: pY466 cortactin
(cortactin-TagRFP)
MW Marker
E
Degradation Area (Normalized)

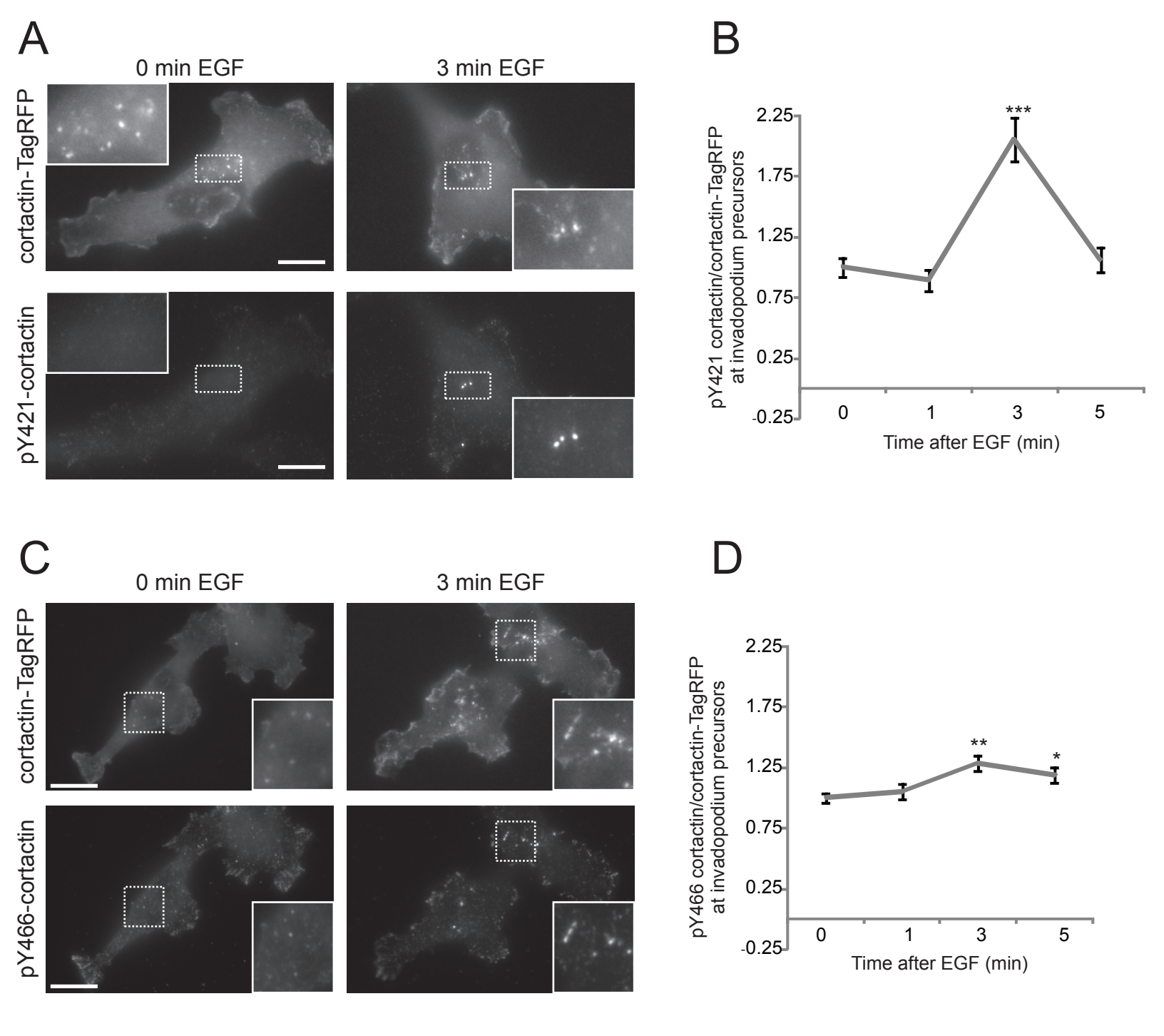
A
0 min EGF
3 min EGF
cortactin-TagRFP
pY421-cortactin
B
pY421 cortactin/cortactin-TagRFP at invadopodium precursors
2.25
1.75
1.25
0.75
0.25
-0.25
***
0
1
3
5
Time after EGF (min)
C
0 min EGF
3 min EGF
cortactin-TagRFP
pY466-cortactin
D
pY466 cortactin/cortactin-TagRFP at invadopodium precursors
2.25
1.75
1.25
0.75
0.25
-0.25
**
*
0
1
3
5
Time after EGF (min)

A

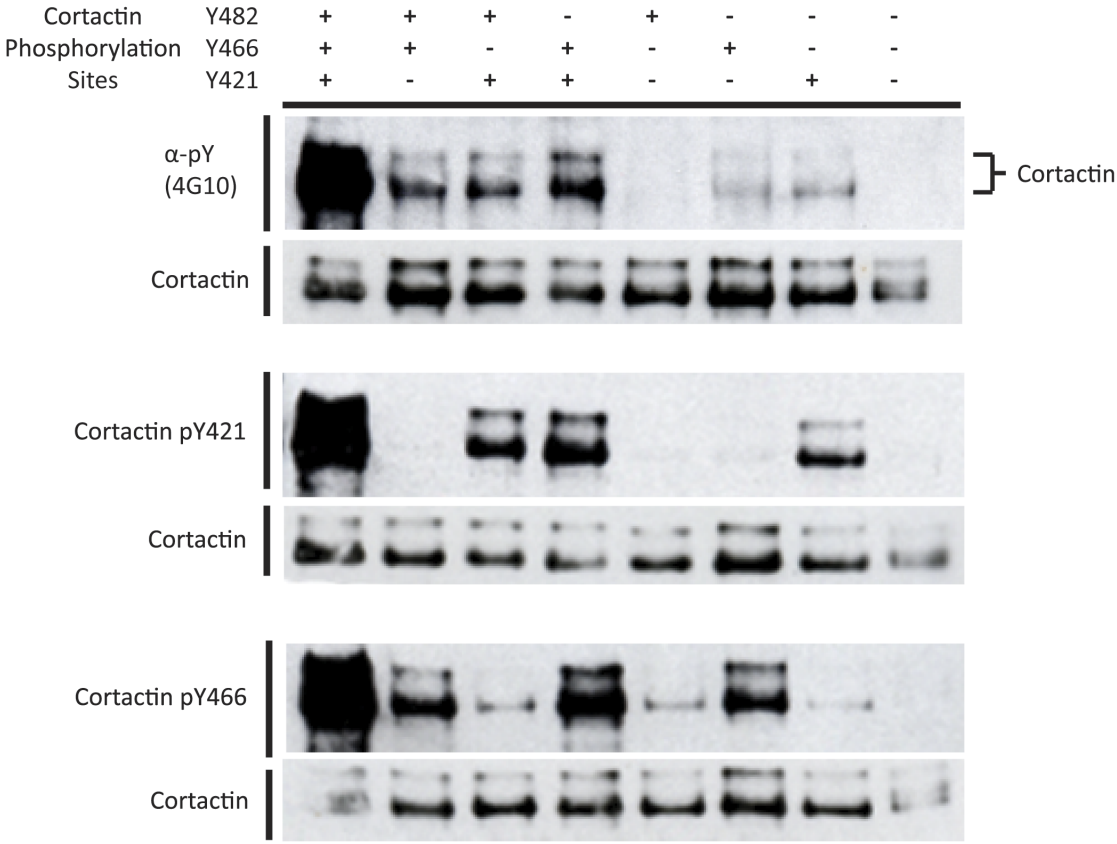
Cortactin Phosphorylation Sites
Y482 + + + - + - - -
Y466 + + - + - + - -
Y421 + - + + - - + -
α-pY (4G10)
Cortactin
Cortactin
Cortactin pY421
Cortactin
Cortactin pY466
Cortactin

B

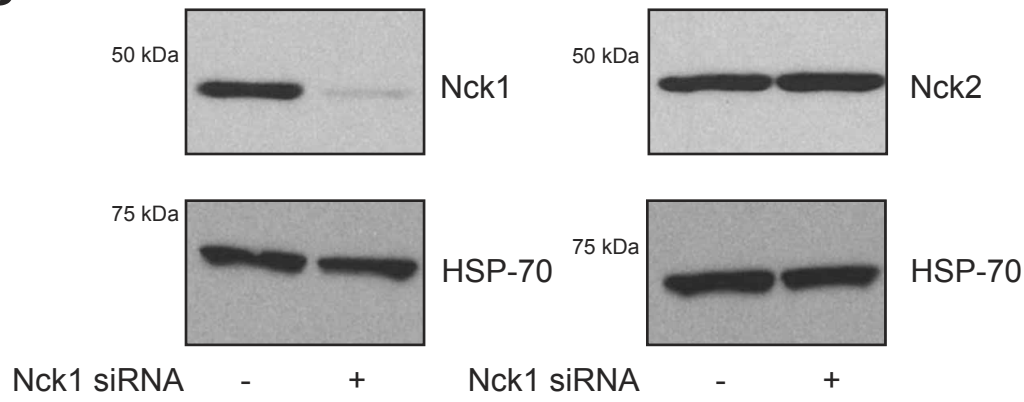
50 kDa
Nck1
50 kDa
Nck2
75 kDa
HSP-70
75 kDa
HSP-70
Nck1 siRNA - +
Nck1 siRNA - +

A

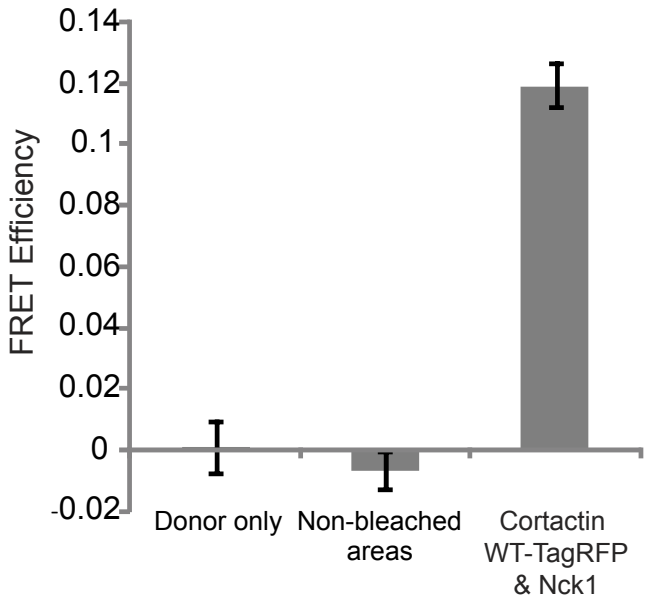
FRET Efficiency
0.14
0.12
0.1
0.08
0.06
0.04
0.02
0
-0.02
Donor only
Non-bleached areas
Cortactin WT-TagRFP & Nck1

B

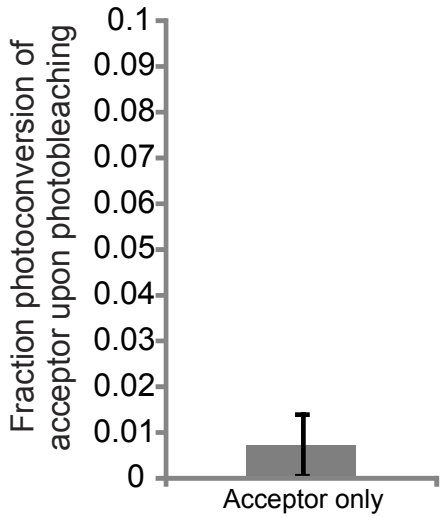
Fraction photoconversion of acceptor upon photobleaching
0.1
0.09
0.08
0.07
0.06
0.05
0.04
0.03
0.02
0.01
0
Acceptor only

C

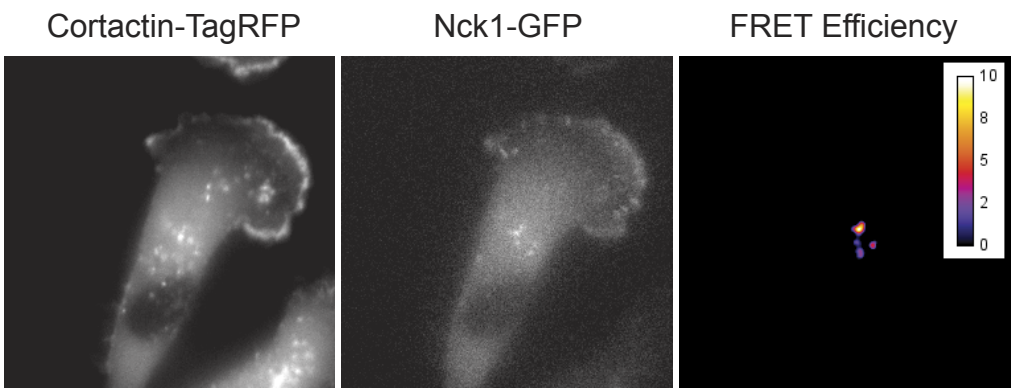
Cortactin-TagRFP
Nck1-GFP
FRET Efficiency
10
8
5
2
0

D

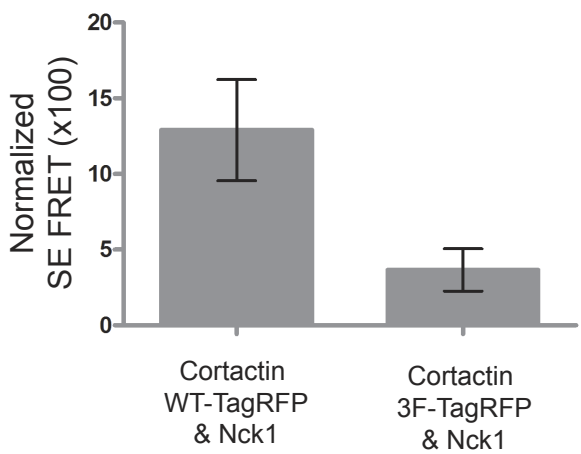
Normalized SE FRET (x100)
20
15
10
5
0
Cortactin WT-TagRFP & Nck1
Cortactin 3F-TagRFP & Nck1

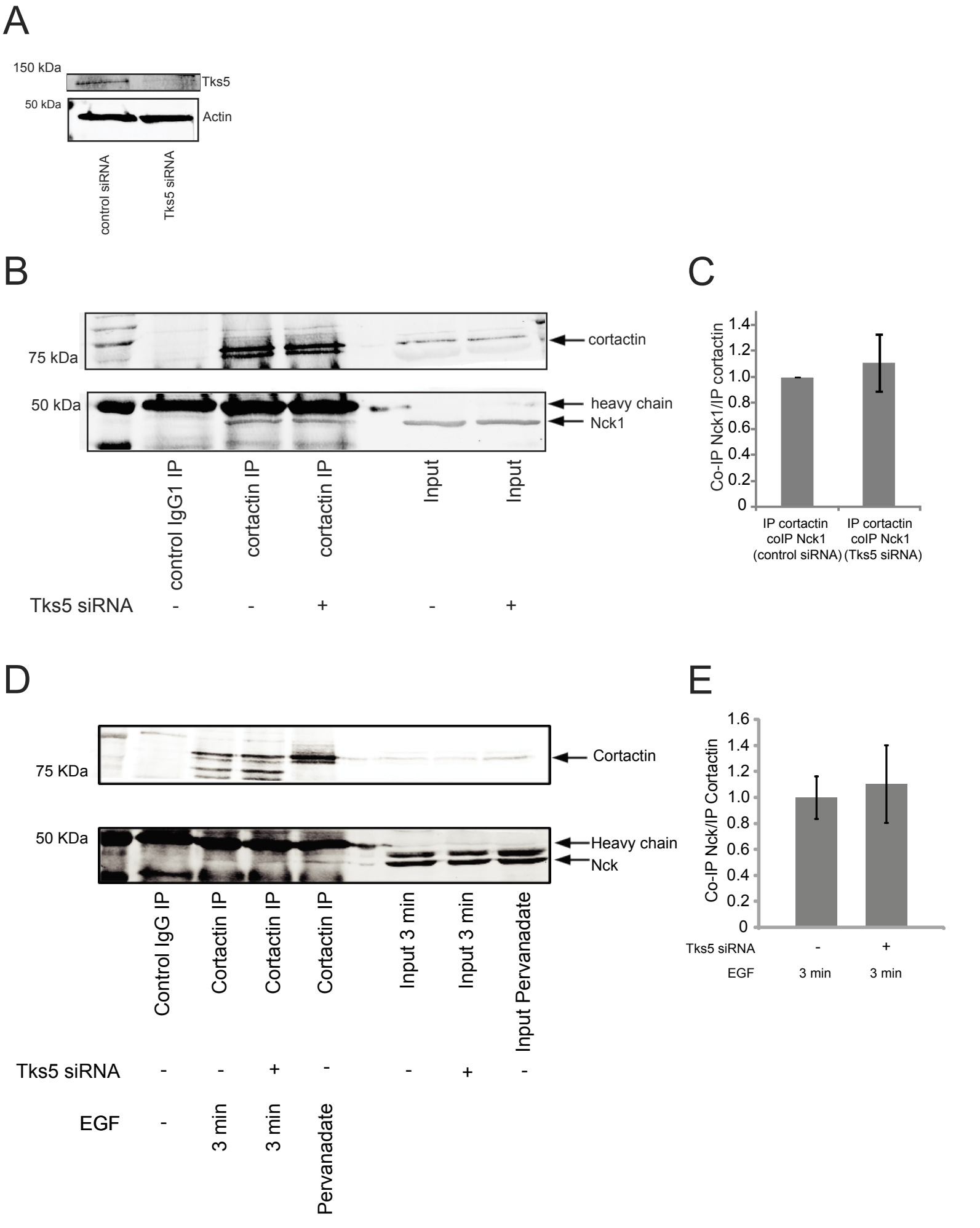

Oser et al. Figure S5